

Research and Development in Connector Systems for Very Large Floating Structures

D. Jiang¹, K.H. Tan², C.M. Wang³, and J. Dai⁴

¹Department of Civil Engineering, School of Science, Nanjing University of Science and Technology, Nanjing 210094, China

²Department of Civil and Environmental Engineering, National University of Singapore, Kent Ridge, Singapore 119260

³School of Civil Engineering, University of Queensland, St Lucia, Queensland 4072, Australia

⁴Department of Civil Engineering and Energy Technology, Oslo Metropolitan University, Oslo 0166, Norway

ABSTRACT

In recent years, Very Large Floating Structures (VLFS) technology has attracted much attention for its sustainable and eco-friendly approach in creating land from the sea. Owing to the massive size, VLFS are usually fabricated as a number of floating modules in shipyards, towed to site and connected on sea. To ensure the functionality of such connected VLFS, effective connector systems are essential. The connector system must address issues related to the relative motion between adjacent modules and be able to sustain forces as a result of wave motion. This paper presents a critical review on the research and development in connector systems for modularized VLFS. Various design concepts for connector systems are first categorized and their working principles outlined. Research studies on hydroelastic analysis of VLFS and the effectiveness of connector systems in reducing the hydroelastic responses and internal stress resultants in connectors are also reviewed. In addition, potential technical challenges on the determination of connector stiffness in practical designs are discussed. Finally, some recommendations and suggestions for future practice are provided.

Keywords: Connector Systems; Hydroelastic Responses; Internal Stress Resultants; Very Large Floating Structures.

1 **1. INTRODUCTION**

2 Very large floating structures (VLFS) have been touted to be a better alternative approach in
3 creating land space on the sea than the traditional land reclamation technique. Their advantages
4 include the freedom in site selection, low construction cost, smaller environmental impact, fast
5 construction, easily scalable, and immunity to flooding (Wang et al., 2015; Xie et al., 2020). Owing
6 to their massive size, VLFS are usually constructed by connecting multiple standardized modules
7 with connector systems; thereby enabling easy construction and transportation. Moreover, a review
8 of past research studies indicates that a monolithic floating structure has to resist enormous
9 bending moments and shear forces that significantly increases the difficulty and complexity of
10 structural design. A connector system is a critical component in the modularized floating structure
11 and should be handled with caution. Many connector designs have been developed and
12 comprehensive research studies were performed on a wide range of connector systems. In this
13 paper, various design concepts for connector systems are first described and categorized according
14 to their working principles. Recent research studies on hydro-elastic responses and structural
15 integrity are then introduced. In addition, the determination of connector stiffness in practical
16 designs is discussed, and suggestions for future engineering practice are provided.

17 **2. TYPES OF CONNECTOR SYSTEMS**

18 **2.1 General**

19 The relative motion between adjacent VLFS modules consists of six components, grouped into

20 translational motions (surge, sway and heave) and rotational motions (pitch, roll and yaw), as
21 shown in Figure 1. Each degree of freedom (DOF) can be rigidly restrained, compliant or fully
22 released. A single connector is usually designed to be compliant to restrain the translational DOF
23 to some extent, and connector systems deployed in VLFS are commonly composed of multiple
24 compliant connectors to restrain more DOFs, as illustrated in Table 1. It can be further inferred
25 that a three-dimensional combination of multiple connectors generally results in a connector
26 system with no unrestrained DOF, denoted as “all-restrained” connector system herein. For
27 instance, VLFS modules connected with horizontal and vertical elements at both short and long
28 sides ideally allow no relative motions. In practice, the margin in each individual connector
29 determines the possible relative motions, and the stiffness of the connector system depends on
30 connector numbers, configurations and materials used.

31 Table 2 compares the key positive and negative aspects of rigid and flexible connector
32 systems. In general, a flexible connector system results in lower connection forces and easier
33 decoupling procedures. By varying the stiffness of individual connectors, the “all-restrained”
34 connector system transits from a fully rigid connection to a fully flexible connection. Connector
35 systems for modules connected with no gap may be categorized into three main types: rigid, semi-
36 rigid and hinge connector systems. A rigid connector system commonly consists of a combination
37 of multiple connectors, whereas a hinge connector system is realized with discrete connectors such
38 as a hinge, a ball joint, and others. The main difference between rigid and hinge connections lies
39 in the transmitted bending moment. The largest action effects in a hinged connector will be the

40 axial and shear forces, while the transmitted moments are negligible. No distinct boundary exists
41 between the rigid and semi-rigid connector systems, but the latter option has a relatively smaller
42 stiffness. Some other connector systems are designed for floating modules with spaces in between,
43 and they include rigid, vertical-free, hinge and flexible connectors.

44 **2.2 Connector Systems for Floating Modules Connected with No Gap**

45 The motions of VLFS are permitted to be within an allowable range. According to various
46 construction principles, alternative design concepts are adopted in developing an “all-restrained”
47 connector system. Table 3 presents typical examples of connector systems developed based on:
48 (1) cable “tensioning”, whereby multiple modules are prestressed with cables or bars; (2) hinge
49 “clicking”, whereby adjacent elements are clicked together with multiple hinges in different DOFs;
50 and (3) tooth “anchoring”, whereby toothed structures are connected with a steel pin.

51 Cable “tensioning” connector system is used to connect floating modules by passing and
52 tensioning cables (or tendons) through internal ducts, by which a larger stiffness can be achieved.
53 This tensioning principle generates well distributed connection forces, but the shear resistance to
54 heave motions could be weak. Hence shear keys may be installed to take care of the transverse
55 shear forces. In practice, cables are not grouted to the sleeves to facilitate future removal when
56 necessary. The cost of cable “tensioning” connector system is low, but the prestressing tendons
57 may have to be destroyed to disassemble the floating structure, and a large part of the connector
58 system will have to be renewed for future repurposing of the floating structure. Rognaas et al.
59 (2001) designed a special connector with steel cables to handle axial tensile forces and hydraulic

60 jacks and elastomeric bearings to provide elastic supports (see Table 3a). The cable compliant
61 technology was also used by Halim to combine adjacent floating modules with different
62 prestressing cable configurations (Table 3b). When the modules are connected only at the upper
63 deck level, this connector system does not effectively transfer internal moments. However, when
64 prestressing cables are arranged at both upper and lower deck levels, flexural resistance can be
65 provided to some extent and the bottom opening scenarios are eliminated (Jiang et al., 2018). The
66 cable “tensioning” connector system has been successfully applied in the Incheon Floating Pier
67 (Table 3c) in 2018 and it has shown good in-service performance so far (Jung et al., 2019). Each
68 fabricated prestressed concrete segment has many connection holes for prestressing bars around
69 the cross section, and double rubber layers were also attached to prevent water penetration during
70 the module connection work. These connection holes were made in advance in the segment
71 fabrication work and closed by temporary rubber water stoppers during the launching of the
72 segment. The stoppers were removed one by one before inserting prestressing bars into the
73 connection holes. All segments were connected to each other by prestressing bars on the sea to
74 form the 200 m long sub-module.

75 Hinge “clicking” connector system is developed with multiple rows of steel piano hinges
76 either in horizontal or vertical alignments. Key protruding steel connections are externally
77 distributed over the sides of the floating module to reduce point load intensity and increase the
78 rigidity. Armin’s connector design (Table 3d) uses steel piano hinges distributed at both top and
79 bottom sides to guarantee sufficient stiffness and effectively transfer bending moments; thereby

80 forming a rigid connector system (Lei, 2007). In contrast, Han's connection (Table 3e) and
81 McDermotts Mobile Offshore Base (MOB) connection (Table 3f) has only one row of hinge
82 connectors and thus they may be considered as a hinge connector system with angular rotations
83 allowed in service (Lei, 2007; Mcallister, 1997). In Armin's design, the lower edges of the joined
84 pontoons tend to open up in sagging condition because the pins are placed only on the deck level,
85 thus tolerance control for the locking pin's holes position is very crucial. When compared to the
86 cable "tensioning" system, steel hinge connections are relatively expensive and are easily damaged
87 in severe sea conditions due to fatigue and durability issues. Besides, it is difficult for inspection
88 or maintenance once steel piano hinges are clicked, thus the costs for replacement of the steel
89 connectors would be high.

90 The tooth "anchoring" connector system is commonly made of protruding teeth attached
91 on sides of adjacent floating modules, which are shoved or slid in place and locked by steel bars
92 or bolts. The large protruding teeth are not easily damaged during coupling, but may hinder the
93 coupling procedure. Bolting technology requires regular monitoring of the bolt torque as it may
94 loosen over time. The tooth "anchoring" connector system is able to bear high internal force in
95 service and it is rather easy for disassembling the floating modules by pulling out the steel bar.
96 Bargeco's connector design (Table 3g) consists of male and female coupling members that can
97 connected with a wedge engagement (Yoon and Boldbaatar, 2013). Similarly, Gardner's design
98 (Table 3h) aligns adjacent pontoons with two coupling members and an elongated connecting
99 member fitting into a recess. Both connector designs have limited tensile strength and require high

100 tolerance control for assembly. Bargeco’s connector demands the mating modules to be even and
101 heel perfectly, which is not practical and may only suitable for calm water condition. Gardner’s
102 design can lock both top and bottom of the connector theoretically, but it is hard to achieve in
103 practice because of tolerances of components and assembly. Tooth “anchoring” technique has been
104 practically used in the connecting system of Floating Performance Stage at the Marina Bay in
105 Singapore. A special square-shaped connector unit made of high tensile steel is designed to connect
106 to the corners of four surrounding floating platforms (Wang et al., 2015). The hollow edges of the
107 connector unit slip into the tapered wedges, and coupling members are kept in place by twelve
108 distributed detachable steel locking pins. The connector system that eventuated required the
109 pontoon modules to be joined at the corners using a floating corner connector and along the mating
110 edges with side connectors (5 along the longer edge and 2 along the shorter edge) (Table 3i). In
111 general, the tooth “anchoring” connector system can be very stiff when subjected to transverse
112 compression, but gaps are needed to insert the steel bar during the coupling process.

113 Figure 2 shows some other connector systems that use bolts or bars to lock adjacent
114 modules without protruding teeth. Au-Yeong proposed connector assemblies that comprise two
115 housings mounted on adjacent floating modules and one movable connector element, as shown in
116 Figure 2a. The connection is established by shifting the connector element from one housing to
117 the other and securing it by horizontal latches at the top and vertical pins at the bottom. In practice,
118 the tolerance between the latch pin and hole has to be large enough for successfully latching all
119 the connector elements with housings, which may result in loose connection and creates gap

120 movements between adjacent modules. A special type of rigid connector system, known as
121 Frictional Locking Connector, was developed by Han-Ocean (Yoon and Boldbaatar, 2013), in
122 which locking bars were dropped in directed recesses of the two coupling parts to secure the
123 connection between floating units. Both designs avoid shoving or sliding of protruding teeth, but
124 a high tolerance control is required for the assembly. Wilkins (2002) patented a connector system
125 with tapered fingers attached on floating modules, as shown in Figure 2c. The male finger
126 assembly includes a casing configured with a camshaft, cams, and connector bodies. The cams are
127 scalloped to prevent the connector bodies from turning the camshafts when they are under loads
128 in a locked position. A similar casing configuration with no moving parts is used for the female
129 finger assembly. Female fingers are preferably placed along one side of the floating module and
130 separated enough so that a male finger may fit flush within the two female fingers.

131 As described above, tooth “anchoring” connector systems can be very strong in resisting
132 transverse compression, but they have limited tensile resistance and require high tolerances during
133 the coupling process. In order to overcome this, a new design of rigid connector system, hereby
134 termed “Prestressed Concrete Shear Key Connection (PCSKC)”, has been developed by the
135 authors. The proposed connection combines the use of tooth “anchoring” and cable “tensioning”
136 approaches. Figure 3 illustrates the proposed PCSKC for the connection of two-modular concrete
137 floating structures. The adjacent floating modules are designed with thicker side walls and
138 connected with prestressed bars at both the top and bottom of the modules, which resist axial
139 tensile forces and provide flexural moment resistance. Shear keys (Figure 3b) are arranged along

140 the interface between two modules to withstand vertical shear forces. The assembly of floating
141 modules using PCSKC requires little tolerance to be provided for installation purpose. In addition,
142 the connection stiffness can be adjusted by varying the shear key arrangements, amount of
143 prestressed bars as well as prestressing forces.

144 **2.3 Connector Systems for Floating Modules with Space in Between**

145 In engineering practices, large floating structures are occasionally made of several modules with
146 space in between so as to improve mobility. In such cases, the rigidity of connector systems is
147 designed in accordance with different practical situations, including rigid connector system,
148 vertical-free connector system, hinge connector system and fully flexible connector system. For
149 instance, the US Navy's Mobile Offshore Base (MOB) platform requires rigid connected modules
150 to accommodate aircraft take-off and landing, whilst fully flexible connector systems that allow
151 sway or surge motions are used for transport reasons, e.g. ducts, cables, or pedestrian bridges
152 connecting to shore.

153 Brown and Root designed a rigid connector system that combines semi-submersible
154 modules in MOB based on in-operation Tension Leg Platform (TLP) connections and ABB Vetco
155 Grey latching system (Ramsamooj and Shugar, 2002). Figure 4 shows the conceptual design of
156 rigidly connected semi-submersible MOB modules and latching interface. Each connector
157 comprises male and female halves, made of thin-walled steel tubing. Each half pivots on a 3.66 m
158 diameter tube, and is able to move or slide on the pivot tube via hydraulic cylinders.

159 Vertical-free connector systems, as shown in Figure 5, are used when surge and sway motions

160 are to be prevented. They can be categorized as “rotation allowing” and “rotation restricting”
161 connections. The vertical-free rotation-free connection (Figure 5a) is made of tubes and rods with
162 horizontal transverse bolts/pens and fixed holes. The sway motion is prevented by clamping the
163 connection elements in the horizontal plane, while the heave motion is allowed since only one set
164 of tubes and rods is used in the horizontal plane. The vertical-free rotation-resistant connection
165 (Figure 5b) uses tubes and rods with horizontal transverse bolts/pens with ends sliding in vertical
166 slots. Diagonal connection elements are used in both horizontal and vertical planes, which can
167 effectively restrict the rotational motions. In a similar manner, hinge connector systems can be
168 realised by using horizontal transverse bolt/pen connections as shown in Figure 6.

169 Flexible connector system is used where floating structures are moored and other relative
170 movements are allowed. Xu et al. (2014) proposed a conceptual design of flexible connector with
171 trapezoidal rubbers and cables, as illustrated in Figure 7. The rubber was mainly used to constrain
172 the longitudinal motion between adjacent modules when compression forces occur. The cable is
173 used to constrain the longitudinal motion between adjacent modules when tension forces occur.
174 Very limited moment and shear force resistances can be provided by such a flexible connector
175 system.

176 **3. RESEARCH STUDIES ON CONNECTOR SYSTEMS**

177 **3.1 Hydroelasticity Theories and Analysis Approaches**

178 VLFS behaves elastically under wave actions because of its large horizontal dimensions as

179 compared to the wavelength, and its small bending rigidity. The response of VLFS cannot be solely
180 described by rigid body motions using conventional hydrodynamic analysis, as the interaction
181 between elastic deformations and the surrounding flow field must be taken into account.
182 Furthermore, for VLFS consisting of multiple interconnected floating modules, the hydroelastic
183 response directly affects the nature and magnitude of internal forces acting on the connectors as
184 well as the overall structural integrity. Thus, a study based on hydroelasticity is essential to verify
185 the serviceability and strength of VLFS.

186 Figure 8 presents an overall view of theories, numerical methods and physical models for the
187 performance evaluation of VLFS. The hydroelastic behavior has been thoroughly studied for ships
188 and floating structures employing potential flow solvers based on: (i) two-dimensional (2D) linear
189 theories (Betts et al., 1977; Bishop and Price, 1977; Jørgen and Mansour, 2002); (ii) 2D nonlinear
190 theories (Juncher and Terndrup, 1979); (iii) three-dimensional (3D) linear theories (Bishop et al.,
191 1986); and (iv) 3D nonlinear theories (Wu et al., 1997; Chen et al., 2003; Chen et al., 2006; Lee et
192 al., 2016). VLFS is frequently simplified as a floating beam or a floating plate model in the analysis,
193 and hydroelastic formulations have been developed through the application of strip theory and
194 Green's function method (Fu et al., 2007). In order to reduce computational effort and time,
195 hydroelastic analysis is commonly carried out in the frequency domain by assuming a linear
196 response. Nonlinear quadratic strip theories formulated in the frequency domain may be used to
197 predict wave loads and structure responses in moderate seas (Juncher and Terndrup, 1979).

198 When nonlinear characteristics of the fluid and structure are taken into consideration or when

199 transient responses are of concern, the frequency domain analysis is not applicable. This happens
200 in some situations such as slamming impact pressures and excessive structural deformations due
201 to airplane landings/take-offs. Under such circumstances, the time domain approach is necessary
202 for solution but it requires intensive computational costs (Feng and Bai, 2017; Nematbakhsh et al.,
203 2017). Commonly-used approaches for the time domain analysis of VLFS includes the direct
204 integration method (Watanabe et al., 1998; Liu, and Sakai, 2002) and the Fourier transform method
205 (Kashiwagi, 2000; Kashiwagi, 2004; Endo, 2000; Ohmatsu, 2005). Liu and Sakai (2002)
206 developed a hybrid approach, by which the boundary element method (BEM) is used to evaluate
207 the fluid motion while the finite element method (FEM) is to calculate the elastic deformation of
208 the floating structure.

209 Kashiwagi (2004) used the time-domain mode-expansion method to assess additional drag
210 forces on airplane due to elastic deformation of the floating runway. Wu and Cui (2009) elucidated
211 various 3D hydroelasticity theories ranging from linear frequency domain analyses to nonlinear
212 time domain analyses. Comparisons between frequency domain and time domain solutions
213 indicated that discrepancies exist for the case of anti-symmetric responses, where time-domain
214 analyses agree better with experimental measurements (Kim et al. 2009). It is worth mentioning
215 that the computational fluid dynamic (CFD) has gained popularity because of its accurate
216 representation of Navier-Stokes equations and ability to handle viscous effects and vortex
217 formations, but intensive computational costs are required (Wang and Tay, 2011; Lee et al., 2003;
218 Lakshmyanarayana and Temarel, 2019). CFD method will not be described in detail herein.

219 Two main numerical methods have been developed to implement the hydroelastic analysis:
220 direct method and mode superposition method. In the direct method, one solves the equation of
221 motion directly with all nodes of the discretized structural system (Namba and Ohkusu, 1999;
222 Khabakhpasheva and Korobkin, 2002; Taylor, 2007; Ohkusu and Namba, 2004; Kim et al., 2007).
223 In particular, Kashiwagi (1998a, b) used the B-spline function to represent both the wave pressure
224 and the elastic deflections. The mode superposition method introduces the generalized flexible
225 modes apart from six rigid-body modes to describe the structural deformations and decomposes
226 the hydroelastic problem into diffraction and radiation problems for each mode (Wu et al., 1995;
227 Senjanovic et al., 2008). The generalized flexible modes require the determination of
228 corresponding mode shapes of VLFS, which can be achieved through either analytical modal
229 functions or FEM eigenvalue analysis. While analytical solutions are only available for structures
230 with simple geometries (Bishop and Price, 1979; Newman, 1994), the FEM approach is capable
231 of modeling structures with complex geometries or assembled by connecting floating modules.
232 Moreover, FEM eigenvalue analysis is able to consider symmetric and anti-symmetric modes
233 simultaneously, as well as 3D structural deformations.

234 The mode superposition method can be further divided into “wet” mode (Loukogeorgaki et
235 al., 2012) and “dry” mode (Fu et al., 2007; Loukogeorgaki et al. 2008) approaches depending on
236 whether the surrounding fluid effect (added mass and hydrostatic-gravitational stiffness) is taken
237 into account in the calculation of VLFS mode shapes. The “wet” mode approach can be more
238 computationally expensive with the inclusion of the surrounding fluid effect. However, dynamic

239 characteristics calculated from the “wet” mode approach can represent the real physical problem
240 better by correctly considering the total mass and stiffness matrices. In addition, the coupling
241 between the ‘dry’ mode shapes of the rigid body modes and the generalized flexible modes, as well
242 as of the generalized flexible modes themselves can be considered when computing the ‘wet’ mode
243 shapes (Loukogeorgaki et al., 2012). It is noted that the utilization of analytical modal functions is
244 considered as a “dry” mode approach, while the FEM eigenvalue analysis can be applied in either
245 the “dry” mode approach (Riggs et al., 2000; Fu et al., 2005; Senjanovic et al., 2008a; Senjanovic
246 et al., 2008b) or the “wet” mode approach (Michailides et al., 2013).

247 In practice, VLFS are usually constructed by connecting multiple standardized modules with
248 connector systems from the viewpoints of easy construction, transportation and deployment
249 (Watanabe et al., 2004). The effect of both flexibility of the structure and the existence of the
250 connectors should be considered to properly evaluate the hydroelastic performance of
251 interconnected multi-modular VLFS. Both floating modules and connector systems can be
252 modelled as either rigid or flexible (including hinges) in the hydroelastic analysis, resulting in four
253 main types of model: rigid module and rigid connector (RMRC), rigid module and flexible
254 connector (RMFC), flexible module and rigid connector (FMRC) and flexible module and flexible
255 connector (FMFC) (Fu et al., 2007). In particular, RMFC model was used by many researchers to
256 predict the hydroelastic responses of VLFS (Wang et al., 1991; Riggs and Ertekin, 1993; Riggs et
257 al., 1999; Wei et al., 2017; Wei et al., 2018).

258 Riggs et al. (2000) compared the use of RMFC and FMFC models in hydroelastic analysis,

259 and found that the effect of module elasticity in the FMFC model can be reproduced in a RMFC
260 model by changing the connection stiffness to match the natural frequencies and mode shapes of
261 the two models. To study hinge-connected floating structures with the modal superposition method,
262 Newman (1997) defined hinge rigid body modes to represent relative motions between floating
263 modules. When the direct method is employed, translational and rotational stiffness are specified
264 for connector systems at the continuity point of interconnected floating modules, and structural
265 mass and stiffness matrices are updated accordingly. For simple hinge connections, rotational
266 stiffness is set to be zero.

267 In the past two decades, the RMFC model has been adopted by many Chinese researchers to
268 predict hydrodynamic responses and connector loads of VLFS. Wang et al. (2002) developed a
269 time sequence analysis method based on the assumption of rigid modules and flexible connectors
270 to study the linear wave-induced response of MOB. Yu et al. (2003; 2004) used RMFC model to
271 study the dynamic responses of MOB connectors and further investigate the effects of connector
272 stiffness, multiple modules interaction, wave angles and sea states on the MOB module motions
273 and connector loads. Yu et al. (2006a; 2006b) applied RMFC model to determine the
274 hydrodynamic responses of the floating trestle in seawaters with finite depth, which were further
275 verified by comparing with spectrometric analysis result and the experimental test result. Liu et al.
276 (2014) further adopted the RMFC model to analyze the dynamic responses of connectors in VLFS
277 with a shallow draft and concluded that the shallow water effect may increase relative motions
278 between floating modules, leading to a higher vertical connector load intensity.

279 Experimental investigations related to interconnected floating modules based on scaled
280 physical models are necessary to practically assess the overall performance and forces in the
281 connector system, and also to verify numerical analysis approaches (Diamantoulaki et al., 2008).
282 Martinelli et al. (2008) carried out 3D experimental tests on I-shaped and J-shaped floating
283 modules connected with tie rods to study effects of module layout and wave obliqueness on the
284 effectiveness of floating breakwaters. Peña et al. (2011) and Ferreras et al. (2014) implemented
285 experimental investigations on π -type floating modules that are connected with flexible connectors
286 (steel cables through cylindrical neoprene) to explore the connectors' forces of VLFS, including
287 horizontal and vertical shear forces and associated moments. Loukogeorgaki et al. (2014)
288 performed 3D experimental tests on an array of multiple floating box-type modules connected with
289 flexible connectors (coated wire rope) to assess connectors' internal forces under the action of both
290 regular and irregular perpendicular and oblique incident waves. Ding et al. (2019) performed
291 model tests on a 3-module VLFS and an 8-module semi-submersible-type VLFS in two simulated
292 shallow sea regions to investigate the hydroelastic responses of VLFS deployed near islands and
293 reefs in shallow sea. The aforementioned physical model studies effectively evaluate the influences
294 of module geometries, environmental conditions and connection types on structural responses and
295 connecting forces, and also helps to verify analytical and numerical solutions.

296 **3.2 Hydroelastic Responses**

297 VLFS is required to satisfy the functional and operational requirements in practice, such as
298 tolerance on the structure motions and structural internal forces. All these criteria are directly

299 related to the hydroelastic response, and it is desirable to reduce the response magnitude as much
300 as possible to ensure the safety and serviceability of VLFS.

301 Many research studies have been performed to evaluate the effect of the connector
302 characteristics on the hydroelastic response of VLFS considering either hinge-type connectors
303 (Lee and Newman, 2000; Xia et al., 2000) or flexible connectors (Fu et al., 2007; Loukogeorgaki
304 et al., 2012). The main responses discussed herein are: (i) vertical deflections; and (ii) internal
305 forces. Lee and Newman (2000) and Teng et al. (2014) investigated rigid floating modules inter-
306 connected with hinge connectors, while Yoon et al. (2014) and Zhao et al. (2015) evaluated the
307 performance of flexible floating modules connected with hinged joints.

308 Figure 9 shows dimensionless vertical deflection and bending moments of floating plate
309 structures with multiple hinge connections, obtained by Yoon et al. (2014) who used the hybrid
310 BEM-FEM method. As the number of hinge connections increases, vertical deflections in the
311 floating plate increase and peak values occur at hinge connections, while bending moments reduce
312 in general and maximum values locate around the centre between adjacent hinges. Note that
313 maximum moment of single-hinge plate is larger than that of the monolithic plate, indicating that
314 the use of hinge connections is not always beneficial in reducing the maximum bending moment.

315 Riggs et al. (2000) implemented hydroelastic analysis of VLFS consisting of rigid modules
316 interconnected with flexible connectors, while Fu et al. (2007) used 3D linear hydroelastic theory
317 to predict the response of flexible floating modules interconnected with flexible connectors.
318 Figure 10 presents vertical deflection profiles and bending moments of a flexible floating plate

319 interconnected with flexible connectors for different rotational stiffness (k_{rot}) (Riggs et al., 2000).
320 In the figure, w represents the calculated deflection value, while symbol, A , in the y axis indicates
321 wave amplitude, where $A = H/2$, and H is the wave height. It is seen that the vertical displacement
322 amplitude decreases as the rotational stiffness increases and the deflection profile of the floating
323 plate interconnected with stiffer connectors approaches the experimental results of continuous
324 structures. Also, the rotational stiffness of the connector system has a greater effect on the regions
325 near the connector. In terms of bending moments, the value at the connector system gradually
326 decreases to zero as the rotational stiffness reduces. On the other hand, the bending moment within
327 the upstream and downstream modules will increase slightly.

328 Xia et al. (2000) evaluated the hydroelastic behaviour of articulated plates interconnected
329 with vertical and rotational springs with a variation of stiffness value from zero to infinity that
330 represent welded joints during the assembling process. The displacement at the connectors is found
331 to be larger than that on the plate, and an increase in the spring stiffness is favourable in reducing
332 the connector motions. The bending moments and shear forces at the connectors are independent
333 of the stiffness of the vertical and rotational springs, respectively.

334 In the aforementioned studies, the number and stiffness values of connections are
335 artificially specified by researchers. Wang et al. (2009) and Riyansyah et al. (2010) proposed the
336 use of a compliance parameter χ (defined in Equation (1)) in determining the optimal rotational
337 stiffness parameter, ξ , and number of semi-rigid connectors, n , to minimize the hydroelastic
338 responses of longish VLFS. A minimum value of compliance parameter is desirable and it is

339 equivalent to a stiff beam acting against wave action.

$$340 \quad \chi = \frac{1}{A\rho L} \int_{-L/2}^{L/2} |p||w| dx \quad (1)$$

341 where A is the wave amplitude, ρ the mass density of water, L the floating beam length, p the
342 hydrodynamic pressure, and w the deflection of the floating beam. Figure 11 compares
343 hydroelastic responses of floating beams with multiple optimally designed semi-rigid connections
344 and with rigid connections. Semi-rigid connections with appropriate stiffness and inserted at
345 suitable locations are found to be more effective in reducing the vertical displacement as compared
346 with rigid or hinge connections. The compliance parameter was observed to reduce by using a
347 moderate number of connector systems, i.e., $n=3-7$. Further increase in number of connections
348 does not result in a significant reduction in the value of the compliance parameter.

349 **3.3 Internal Forces in Connectors**

350 The structural integrity of VLFS under wave action strongly depends on the induced internal forces
351 in the connectors. Up to now, limited research studies had been carried out on the numerical
352 evaluation of the internal forces and effects of various design parameters, such as stiffness of
353 connectors, module layout, shallow water effect and incident wave period (Kim et al., 2007; Liu
354 et al., 2014; Michailides et al., 2013; Newman, 1997; Qi et al., 2017; Yu et al., 2003; Yu et al.,
355 2004).

356 Past research studies indicate that rigid connectors generally lead to high load intensity,
357 whilst the use of hinge connectors can effectively reduce the magnitude of connecting forces (Gao
358 et al., 2011; Gao et al., 2013; Dai et al., 2018; Jiang et al., 2019). Therefore, connector systems

359 with a certain degree of flexibility are usually adopted in designs of VLFS. Specifically, Newman
360 (1997) computed the shear forces acting on the hinge connectors of floating structures, and
361 analysed the influence of the number of floating modules on the forces in hinge connectors. On
362 the other hand, Kim et al. (2007) evaluated the bending moments and the shear forces at flexible
363 connections of VLFS assembled of modules, and concluded that the internal forces in connectors
364 of side-by-side arranged VLFS modules generally increase as the connection stiffness and heading
365 angle increase. Qi et al. (2017) studied the relationship between the connector load and rigidity by
366 computing the dynamic responses of flexible connectors in a VLFS with different combinations of
367 transverse, longitudinal and vertical rigidities. Analysis results show that whether the transverse
368 rigidity is high or low, there exists a combination of longitudinal and vertical rigidity that results
369 in the peak connector load. Zhao et al. (2019) further provided optimal stiffness values in three
370 directions of flexible connectors for multi-modular floating systems in different sea conditions.

371 Apart from the connector stiffness, incident wave characteristics also cause significant effects
372 on connector forces of VLFS. Yu et al. (2003; 2004) conducted numerical analyses of MOB
373 connector loads on the basis of a RMFC model. The results indicate that the longitudinal connector
374 loads are much larger than the lateral and vertical loads. Besides, the wave headings significantly
375 affected the forces between modules, and the longitudinal load of the connector reached its
376 maximum with a 75° wave direction. It is suggested to keep the angle between the MOB and wave
377 direction less than 45° and to avoid unrealistically large connector loads.

378 Ding et al. (2019) performed a model test on an 8-module semi-submersible-type VLFS with
379 specified connector stiffness of 4.60×10^6 N/m, 6.55×10^6 N/m and 9.78×10^6 N/m in three directions.
380 Figure 12 presents the variations of connecting forces along the length of the VLFS model from
381 connectors C1, C3 to C13. Three frequencies representing short, medium and long regular waves,
382 that is, 0.897 rad/s ($T = 7$ s), 0.483 rad/s ($T = 13$ s) and 0.209 rad/s ($T = 30$ s) were considered. The
383 distribution of internal forces is significantly dependent on the frequency of incoming waves. Axial
384 forces, F_x , for connectors in the middle of the longish VLFS are generally greater than those at the
385 two end parts, but no consistent pattern is observed for shear forces, F_y .

386 Loukogeorgaki et al. (2014) implemented 3D experiments to assess the internal forces in
387 connectors of multiple floating box-type modules with flexible connectors, under wave actions of
388 different characteristics (wave obliquity, wave period and wave height). Figure 13 shows the
389 variation of internal forces with the change of incident wave frequency and wave steepness. Test
390 results showed that the wave obliquity and wave height affect forces mainly in the low frequency
391 range ($6 \text{ rad/s} < \omega < 9 \text{ rad/s}$). Contrary to Ding's findings, it is seen from Figure 13 that the increase
392 in incident wave frequency generally leads to the decrease in axial and shear forces, which may
393 attribute to a relatively higher wave frequency and a shorter structural length. Besides, the increase
394 in incident wave steepness (H/L) results in the increase of these forces, especially in the low
395 frequency range. For the same wave height and period, the increase of wave obliquity from 60° to
396 90° leads to a decrease in internal forces, resulting in a more efficient floating structure in terms
397 of both functionality and structural integrity.

398 Most research studies were conducted on VLFS with modules connected in the transverse
399 direction only. Michailides et al. (2013) considered VLFS consisting of a grid of floating modules
400 flexibly connected in two directions, and identified the optimal module layout and connectors'
401 rotational stiffness. Figure 14 presents the variation of connector internal forces as a function of
402 incident wave frequencies for a 3×3 grid type floating structure with wave angle $\beta = 0^\circ$. The
403 increase in connector rotational stiffness from K_{R1} and K_{R2} to K_{R3} results in a decrease of the peak
404 axial forces and shear forces. Additionally, a larger rotational stiffness K_{R3} leads to larger moments
405 in X direction, $M_{y,Xc}$.

406 Figure 15 compares the axial forces in X direction, $F_{x,Xc}$ as a function of incident wave
407 frequency for different module layout and various rotational stiffness values. The change of the
408 module number and layout directly affects connectors' internal loads. Specifically, a 1×2 grid
409 structure has the largest maximum axial force, $F_{x,Xc}$, compared to structures with other grid layouts.
410 For all cases, the axial forces $F_{x,Xc}$ was the same and small regardless of connector stiffness when
411 the incident wave frequency $\omega \geq 2.72$ rad/s.

412 To further investigate the application of a combination of hinge and rigid connectors in
413 floating structures and their effects on the connector forces, a comprehensive experimental model
414 test program was conducted by the authors at the National University of Singapore (NUS)
415 Hydraulics Laboratory. Figure 16a shows three floating module layouts tested in the wave basin,
416 including one-line system, 2×4 grid system and 3×3 grid system. In the one-line system, two
417 proposed connector types (rigid or hinge) were applied for the outermost connector. Similarly,

418 rigid and hinge connector systems were explored in 2×4 and 3×3 grid module layouts as
419 described in Figure 16a. Note that the first two modules in the one-line system served as “a floating
420 bridge” to connect the longish floating structure with the onshore quay boundary. Figure 16 b–d
421 presents the maximum bending moments of three module layouts under 100-year irregular wave
422 with a heading angle of 0 degree. In general, the moments can be effectively reduced with the use
423 of hinge connectors, especially for 2×4 and 3×3 grid systems. However, the motions of the
424 hinge-connected systems were relatively larger, thus a trade-off needs to be considered between
425 connecting loads and structural motions in the design of connector system. In addition, a longish
426 VLFS (one-line system) may sustain larger connecting forces compared to the floating structure
427 with smaller length-to-width ratios (that is, 2×4 and 3×3 grid systems).

428 Liu et al. (2014) studied the shallow water effect on the dynamic characteristics of connectors.
429 It shows that the vertical connector load tends to be amplified for a VLFS with a shallow draft,
430 which should be considered in the engineering design practice. Gu et al. (2015) used the time
431 domain method to determine the connector loads for a VLFS under the combined action of wave
432 loads and ship impact loads. Under impact loads, high-frequency oscillations in the time history
433 curve of the connector load are observed. Under different wave headings, the maximum magnitude
434 of the connector load is found to occur in the X direction. An oscillatory connector load is observed
435 in the Y direction with a wave heading of 75° .

436 **3.4 DISCUSSION**

437 **3.4.1 Determination of Connector Stiffness**

438 Assessment of hydroelastic responses combined with determination of connector forces represents
439 a key element towards an integrated design of VLFS. Based on extensive review work presented
440 above, it is concluded that various factors significantly affect the performance of VLFS in terms
441 of operational design requirements and structural integrity. These include the variation in
442 connector stiffness, geometrical dimensions, and grid type of floating structures and wave field
443 characteristics (that is, wave obliquity, wave period, wave height, etc.), of which the connection
444 stiffness is particularly important.

445 In general, the use of rigid connector systems induces relatively smaller structural motions
446 but extremely higher internal loads when compared to hinge connectors. To achieve a balance
447 between load and motion responses, flexible connectors that utilize compliant materials such as
448 rubber, spring, and cable, have been used in practice. However, this results in complex connector
449 system and design, and raises difficulties in quantifying the stiffness accurately, apart from
450 referring it as a semi-rigid connector system. Meanwhile, in the evaluation of hydroelastic
451 responses and connecting forces in VLFS with flexible connectors, researchers usually artificially
452 specify the translational and rotational stiffness from zero to infinity, regardless of their feasibility
453 of the connector system. Under such circumstances, there is a gap between the results of
454 hydroelasticity research and the development of practical connector systems. As part of critical
455 design variables of VLFS, connector characteristics should be defined and selected to satisfy the

456 design objective and operational requirements.

457 Experimental test is an effective way to determine the actual stiffness of a practical VLFS
458 connector system via the load-deformation relationship. China Ship Scientific Research Center has
459 conducted extensive experimental research studies on the strength and behavior of various
460 practical connector systems. Qi et al. (2015) designed a flexible connector system for VLFS with
461 a shallow draft, which is composed of 5 ball-and-spring devices (2 devices in the x direction, 2
462 devices in the z direction and 1 device in the y direction), as shown in Figure 17. Comprehensive
463 static and dynamic load tests were performed to study the rigidity and evaluate the structural safety
464 of the connector design. Test results indicated that the relationship between load and deformation
465 of the flexible connector system remains in the linear range during the test, from which the stiffness
466 value can be obtained. Besides, different load combinations may result in uneven deformations in
467 the 2 ball-and-spring devices in the x direction, which requires special attention in the design.
468 Zhang et al. (2019) explored the use of nylon and rubber materials in the design of a flexible
469 connector. Mechanical properties of the connector system were determined from experimental
470 tests, from which a nonlinear relationship between the load and displacement was observed. The
471 stiffness characteristics and stress magnitudes are found to be significantly influenced by nylon
472 and rubber material properties, which needs to be optimized in the engineering design practice.

473 In the case that the test data of VLFS connector is unavailable, engineers are required to use
474 reasonable stiffness values in the design. Figure 18 shows the flow chart proposed by the authors
475 to determine the connector stiffness for practical designs. The process includes two main parts:

476 hydroelastic analysis and structural analysis. First, the connector stiffness values are assumed
477 according to its characteristics. For instance, the rotational stiffness can be set as a large value for
478 near-rigid connectors, whereas it should be set small for near-hinge connectors. For the
479 translational stiffness, Zhao et al. (2019) has studied the optimal stiffness layout of modularized
480 floating structures using genetic-algorithm-based approach and concluded that the stiffness along
481 the surge motion should be designed relatively soft while the stiffness along the sway and heave
482 motions should be designed relatively hard against shear load. The suggested optimized stiffness
483 in three directions are $k_x = 10^6$ N/m, $k_y = 10^{11}$ N/m and $k_z = 10^{11}$ N/m (where x, y and z represent
484 surge, sway and heave, respectively), which can be used as initial values if no other information is
485 available. With the assumed connector stiffness, and in conjunction with wave field characteristics
486 and structural geometry information, the hydroelastic analysis can be performed on the VLFS to
487 obtain the connector internal forces. Next, a detailed finite element model of the connector systems
488 needs to be established to perform the deformation analysis with the inputs of connector
489 geometries, material properties and connecting forces. The relations between the loading and
490 deformation response are obtained, from which the connector stiffness can be inferred. If this
491 differs from the initial assumed value, the hydroelastic analysis will be carried out for a second
492 round with the obtained stiffness, and the iteration ends when the stiffnesses converge. Shi et al.
493 (2018) claimed that the connector stiffness is related to connecting forces and material nonlinearity,
494 thus several rounds may be needed in the iterative procedure to finalize the actual stiffness values.
495 As the by-product, the strength analysis can also be carried out using the detailed finite element

496 model to check the safety of the connector design under maximum internal loads.

497 **3.4.2 Fatigue Strength**

498 Connector systems of VLFS are subjected to repeated loading conditions throughout the service
499 life due to the cyclic nature of environmental loads, which may result in serious fatigue problems.

500 Although extensive research studies on fatigue analysis and design of marine structures have been
501 conducted, very limited literature were found on fatigue behavior of connector systems specifically
502 (Lotsberg, I. 2016). Ramsamooj et al. (2001; 2002) developed an analytical model to predict the
503 fracture-based fatigue life of VLFS connectors under random wave actions in the marine
504 environment. Besides, a performance function is further defined in terms of the material properties,
505 nominal stress range and inherent defect or starter crack to perform the reliability-based design
506 analysis of the fatigue life of the connectors in MOB. The reliability calculations indicated that
507 relatively lower stress values should be used in the design to meet the fatigue life target reliability
508 level. Wang et al. (2009) predicted the fatigue behavior of the connectors in a floating bridge with
509 employing the local stress–strain approach. It is revealed that the ultimate tensile strength and the
510 sequence of the dynamic loads may significantly influence the fatigue damage of the connectors.
511 More research studies are expected to ensure the safety and economical design of connector
512 systems for VLFS.

513 The China Ship Scientific Research Center studied the fatigue strength of various VLFS
514 connector systems in recent years. Liu (2014) utilized the S-N curve method and theory of fracture

515 mechanics to predict the fatigue life of a connector system. Seven S-N curves were considered,
516 and the effects of wave angles and sea states on the fatigue damage were analyzed. Single-stage
517 Paris law and two-stage Paris law were adopted to calculate the fatigue life of connectors with an
518 initial crack of thirty different sets of sizes and shapes. It is concluded that smaller initial cracks
519 generally lead to slower crack growth speed and longer fatigue life of the connectors. Qi et al.
520 (2017) conducted a model test of a hinge connector, consisting of a nylon sandwich and a pipe
521 shaft strengthened by circular frames to evaluate the fatigue strength and structural stresses of the
522 connector. The fatigue life was evaluated based on theory of the S-N curve and crack propagation
523 separately. The fatigue life and fatigue strength are found to be significantly affected by the load
524 magnitude and wave angle. Zhao et al. (2018) carried out an experimental study on the ultimate
525 strength of the VLFS connector foundation support reinforcing area structure under complex loads.
526 Plastic hinges were observed in the model when subjected to large combined vertical and
527 longitudinal loads. Therefore, the material nonlinearity may be important and should be considered
528 in the analysis and design of connector systems for VLFS.

529 **3.4.3 Active-control Connector System**

530 Since the structural responses and connector forces of modularized VLFS are significantly affected
531 by connector stiffness, Xia et al. (2016) proposed a special active-control connector system with
532 air-springs. The connector stiffness could be adjusted along with the evolution of wave conditions
533 by changing the air pressure inside the air-spring to reduce the oscillation of floating structures.

534 Figure 19a presents adjacent floating modules connected with two parallel air-springs, where
535 symbols δ_1 and δ_2 represent respectively the initial horizontal and vertical distances between two
536 modules. The air-spring configuration is shown in Figure 19b. An in/outlet is reserved for inflating
537 or deflating the air-spring, and rubber bumper is used to cushion the hard impact due to extreme
538 motion. Although the stiffness of connector can be altered by changing the air pressure, it is still
539 difficult to accurately quantify the stiffness for practical design. Moreover, this special active-
540 control connector system is also limited in terms of timeliness and complexity of the sensor signal
541 transmission.

542 **3.4.4 Materials Design of Connector System**

543 Connector systems for VLFS can be designed with different materials such as steel, concrete and
544 composites. The selection of appropriate materials relates to their own strength and advantages,
545 functional requirements and application scenarios of floating structures. Considering its good
546 mechanical properties and light weight, steel is suitable for connector systems in medium-scale
547 floating structures that need to be transported from place to place, such as military pontoons, barges
548 and causeways. On the other hand, concrete is resistant to seawater and keeps maintenance costs
549 low, making it more attractive for connections in large permanent floating structures like
550 breakwaters, piers and jetties.

551 In a seawater environment, a sophisticated connector system can be made of various materials
552 to meet different requirements in practice. Conventional materials (steel and concrete) are

553 commonly used for critical stiff components to ensure the structural integrity of VLFS once
554 adjacent floating modules are joined. Rubber and foam are preferable for flexible components of
555 the connector system to withstand impact loading and absorb kinetic energy of the moving modules,
556 which can effectively dampen and gently decelerate the motion. In a sense, the use of the
557 aforementioned two types of materials with distinctive mechanical properties fulfill two
558 contradicting requirements on the elasticity and rigidity of the connector system. Additionally,
559 steel cables or springs are occasionally used in the connection design to withstand axial tensile
560 forces.

561 Fibre reinforced polymer (FRP) has been increasingly used in a variety of structures in the
562 severe environments. FRP materials exhibit a linear-elastic behavior under tensile loading up to
563 failure without showing any plastic behavior, owning higher tensile strength, but lower Young's
564 modulus, than conventional steel. In general, carbon fibre reinforced polymer (CFRP) shows more
565 favorable behaviors in terms of mechanical characteristics, chloride resistance and anti-moisture
566 compared to FRPs manufactured of other materials, such as glass, aramid, and basalt (Sen et al.
567 1998a, b). Although no existing literature reported the use of CFRP in the connector system for
568 VLFS, CFRP is a preferable substitute for the stiff component (steel block) and flexible component
569 (steel cable) for anti-corrosion purposes. Specifically, ElSafty et al. (2014) evaluated the
570 characteristics of prestressing carbon fiber composite cables (CFCC) in severe environment and
571 concluded that CFCC showed excellent performance, maintaining very high guaranteed tensile
572 strength retention and elastic modulus retention after conditioning for over 7,000 hours in an

573 alkaline solution. Pantelides et al. (2003) reported that CFRP composites with their superior
574 strength and resistance to electrochemical corrosion are a practical alternative for connecting
575 precast concrete members in building structures. It is worth mentioning that mechanical properties,
576 strength and stiffness of FRP decrease significantly with the increase of temperature (Fried, 1995).
577 Therefore, the use of FRP may not be suitable where high temperature is of concern.

578 Durable connector systems that require less intrusive maintenance are highly desirable
579 because it would exhibit longer life spans and thus maximize the use of the VLFS in the seawater
580 environment. Ultrahigh performance concrete (UHPC) has roused great interests in the past
581 decades due to its advantageous material properties, such as high strength, low permeability to
582 water and chemical substance, good chloride penetration resistance, which is believed to have a
583 broader application prospect in marine environments (Li et al., 2020; Shi et al., 2015; Wang et al.,
584 2015). Similar as an FRP material, UHPC has not been applied in the connector system for VLFS
585 at the current stage. However, this new advanced cementitious composite material has been widely
586 used in the design and construction of connections for concrete bridge superstructures. Graybeal
587 (2010) investigated the structural behavior of field-cast UHPC connections for modular bridge
588 deck components via static and cyclic loading tests, and better performances were demonstrated
589 than those of a conventional cast-in-place bridge deck. In Canada, 42 adjacent box-girder bridges
590 were constructed with UHPC shear keys since 2008 (Rahman and McQuaker 2016). Yuan and
591 Graybeal (2016) conducted full-scale tests on the UHPC joints when subjected to over 1 million
592 load structural cycles and 10 thermal load cycles, and research results shown an enhanced strength

593 of the connection filled with UHPC. Based on the experience in bridge engineering, UHPC can be
594 a competitive material for the design of the stiff component (concrete block) in connector systems
595 for VLFS.

596 **3.4.5 Special Considerations**

597 The integration of the wave energy converter (WEC) and VLFS has been conceptually studied by
598 some researchers in recent years, which may bring benefits owing to space-sharing and multiple
599 functions of the integrated system. Nguyen et al. (2019) proposed a raft WEC-type attachment that
600 consists of multiple narrow pontoons connected to the fore of VLFS with hinge connectors and
601 Power Take-Off (PTO) systems. The relative rotation between narrow pontoons and VLFS is
602 utilized for power production, and the hydrodynamic responses of VLFS can be reduced
603 simultaneously. Zhang et al. (2019) and Ren et al. (2019) suggested to embed PTO systems with
604 connectors between adjacent floating modules to utilize the relative rotation for power production.
605 Although no auxiliary pontoons are required for VLFS with embedded PTO systems between
606 modules, the produced power should be limited due to stringent motion requirements of VLFS
607 (e.g. the slope of a floating runway must be less than 1° (Suzuki, 2005)). Most of the studies on
608 converting the wave energy from motions of connector systems for VLFS are still in the conceptual
609 design stage, and several disadvantages has been reported, for example, the power capture factor
610 of WEC-VLFS integrated system is limited for long wave conditions. Therefore, more research
611 work needs to be further conducted to promote the development and maturity of this technique.

612 4. CONCLUDING REMARKS

613 In the next decade and beyond, we shall witness the construction of very large and sustainable
614 floating platforms near congested coastal cities to create space on the adjacent water bodies for
615 urban expansion. With the adoption of modular prefabricated construction approach for VLFS,
616 the design and manufacturing of effective connector systems and careful construction control to
617 safely connect segments on the sea is needed. A literature review on research and development in
618 connector systems for modularized VLFS is presented. Key findings, potential design issues and
619 suggestions for practice are summarized as follows:

- 620 1. Connector systems are categorized into cable “tensioning” connector, hinge “clicking”
621 connector and tooth “anchoring” connector. By combining the tooth “anchoring” and cable
622 “tensioning” technologies, a new design of connector system, PCSKC, is developed and
623 presented herein for easy installation and stiffness adjustment.
- 624 2. Analysis based on hydroelasticity is crucial in the determination of structural responses and
625 connector forces in modularized VLFS. The analysis is usually carried out in the frequency
626 domain assuming linear response for easy computations. However, the time domain method
627 has to be used when nonlinear characteristics of the fluid and structure or transient responses
628 are of concern. Two main numerical methods, direct method and mode superposition method,
629 have been developed for hydroelastic analysis. The latter method can be further divided into
630 “wet” mode and “dry” mode approaches depending on whether the surrounding fluid effect is
631 taken into account.

- 632 3. The effect of both flexibility of the structure and the existence of the connectors should be
633 considered to properly evaluate hydroelastic performance of modularized VLFS. Both floating
634 modules and connector systems may be modeled as either rigid or flexible. This results in four
635 types of model: RMRC, RMFC, FMRC and FMFC. In particular, RMFC model was used by
636 many researchers to predict the hydroelastic responses of VLFS, considering the flexibility of
637 the connector system.
- 638 4. Rigid connectors generally lead to high internal forces, whilst hinge connectors can effectively
639 reduce the connector forces. Thus, practical designs seldom adopt rigid connectors. As the
640 number of hinge connections increases, vertical deflections increase and peak values occur at
641 hinge connections, while bending moments reduce in general and maximum values occurs
642 mid-way between adjacent hinges.
- 643 5. Semi-rigid connectors with appropriate stiffness and installed at suitable locations are found
644 to be more effective in reducing structural responses when compared to fully rigid or hinge
645 connections. Bending moments and shear forces at the connectors are independent of the
646 stiffness of the connector system, respectively.
- 647 6. Besides connector stiffness, geometrical dimensions, grid type, and wave field characteristics
648 also affect the magnitude of connector forces significantly. Hydroelastic analyses are required
649 to assess the internal forces accounting for these parameters. In general, longish VLFS (one-
650 line system) sustains larger connecting forces compared to floating structures with smaller
651 length-to-width ratios.

- 652 7. The stiffness of the flexible connector is of utmost importance because it seriously affects the
653 connector loads and dynamics of the floating platform. To address the inconsistency in the
654 determination of connector stiffness between hydroelasticity research and development of
655 practical connector systems, an iterative procedure is proposed herein to determine the actual
656 stiffness of connector systems using both hydroelastic analysis and finite element structural
657 analysis.
- 658 8. Current methods of analysis involve complicated mathematical models and techniques which
659 are difficult to use. Simplified methods of analysis and models are in dire need for design
660 practice.
- 661 9. CFRP and UHPC can be potential advanced materials in the design of connector systems for
662 VLFS for the considerations of mechanical properties and durability.
- 663 10. More research studies need to be carried out on the fatigue behaviour of connector systems for
664 VLFS to ensure the safety and economical design in the engineering practice.

665 **ACKNOWLEDGEMENT**

666 The first, second and fourth authors gratefully acknowledge the funding supports from the Natural
667 Science Foundation of Jiangsu Province under Grant No. BK20180487, and the National Natural
668 Science Foundation of China (NSFC) under Grant No. 51808292. The third author gratefully
669 acknowledges the funding support from the Australian Research Council under Discovery Project
670 DP170104546 grant.

671 **REFERENCES**

- 672 Betts, C.V., Bishop, R.E.D. and Price W.G., 1977. The symmetric generalised fluid forces applied
673 to a ship in a seaway. *Royal Institution of Naval Architects Supplementary Papers*. 199:265–78.
- 674 Bishop, R.E.D., and Price, W.G., 1977. The generalised antisymmetric fluid forces applied to a
675 ship in a seaway. *International Shipbuilding Progress*. 24:3–14.
- 676 Bishop, R.E.D., and Price, W.G., 1979. Hydroelasticity of ships. Cambridge: Cambridge
677 University Press.
- 678 Bishop R.E.D., Price, W.G. and Wu, Y., 1986. A general linear hydroelasticity theory of floating
679 structures moving in a seaway. *Philos. Trans. R. Soc. Lond., Ser A*. 316:375-426.
- 680 Chen, X., Wu, Y., Cui, W., and Jensen, J. 2006. Review of hydroelasticity theories for global
681 response of marine structures. *Ocean Engineering*, 33(3-4), 439-457.
- 682 Chen, X., Wu, Y., Cui, W. and Tang, X., 2003. Non-linear hydroelastic analysis of a moored
683 floating body. *Ocean Eng.* 30 (8), 965–1003.
- 684 Dai, J., Ang, K. K., and Zhang, C., 2018. Hydroelastic analysis of modular floating barges for
685 hydrocarbon storage facility: energy and geotechnics. *Proceedings of the 1st Vietnam Symposium
686 on Advances in Offshore Engineering*. November 1–3. Hanoi, Vietnam,
- 687 De Rooij, G.V.P., 2006. A Very Large Floating Container Terminal Feasibility Study – Application
688 Possibilities for the Situation in the Netherlands. Master Thesis. Delft University of Technology.
- 689 Diamantoulaki, I., Angelides, D., and Manolis, G., 2008. Performance of pile-restrained flexible
690 floating breakwaters. *Appl Ocean Research*. 30:243–55.
- 691 Ding, J., Wu, Y., Zhou, Y., Li, Z., Tian, C., Wang, X., Zhang, Z. and Liu, X., 2019. A direct coupling
692 analysis method of hydroelastic responses of VLFS in complicated ocean geographical
693 environment. *Journal of Hydrodynamics*. 31:582-93.
- 694 ElSafty, A., Benmokrane, B., Rizkalla, S., Mohamed, H., and Hassan, M. 2014. Degradation
695 assessment of internal continuous fiber reinforcement in concrete environment. Univ. of North
696 Florida. Materials Research Rep. Contract No. BDK82#977-05. Jacksonville. FL: College of
697 Computing. Engineering and Construction.
- 698 Endo, H., 2000. The behaviour of a VLFS and an airplane during takeoff/landing run in wave
699 condition. *Marine Structures*. 13:477–91.
- 700 Feng, X., and Bai, W., 2017. Hydrodynamic analysis of marine multibody systems by a nonlinear
701 coupled model. *J Fluid Struct.* 70:72-101.

702 Ferrerask, J., Peña, E., López, A., and López, F., 2014. Structural performance of a floating
703 breakwater for different mooring line typologies. *J Waterw Port Coastal Ocean Eng.* 140:paper
704 No. 04014007.

705 Fried, J. 1995. Polymer science and technology: introduction to polymer science. New Jersey:
706 Prentice Hall PTR Inc.

707 Fu, S., Cui, W., Chen, X., and Wang, C., 2005. Hydroelastic analysis of a nonlinearly connected
708 floating bridge subjected to moving loads. *Marine Structures.* 18:85–107.

709 Fu, S., Moan, T., Chen, X., and Cui, W., 2007. Hydroelastic Analysis of flexible floating
710 interconnected structures. *Ocean Eng.* 34:1516–31.

711 Gao, R.P., Tay, Z.Y., Wang, C.M. and Koh, C.G., 2011. Hydroelastic response of very large floating
712 structure with a flexible line connection. *Ocean Engineering.* 38:1957-66.

713 Gao, R.P., Wang, C.M. and Koh, C.G., 2013. Reducing hydroelastic response of pontoon-type very
714 large floating structures using flexible connector and gill cells. *Engineering Structures.* 52:372-
715 383.

716 Graybeal, B. A. 2010. Behavior of field-cast ultra-high performance concrete bridge deck
717 connections under cyclic and static structural loading (No. FHWA-HRT-11-023). United States.
718 Federal Highway Administration.

719 Gu, J., Wu, J., Qi, E., Guan, Y., Yuan, Y., 2015. Time domain calculation of connector loads of a
720 very large floating structure[J]. *Journal of Marine Science and Application*, 14(2): 183–188.

721 Jiang D, Tan, K.H., Wang, C.M., Ong, K.C.G., Bra, H., Jin, J., and Kim, M., 2018. Analysis and
722 design of floating prestressed concrete structures in shallow waters. *Marine Structures.* 59:301-
723 320.

724 Jiang, D., Tan, K. H., Dai, J., Ong, K. C. G., and Heng, S., 2019. Structural performance evaluation
725 of innovative prestressed concrete floating fuel storage tanks. *Structural concrete*, 20(1):15-31.

726 Jørgen, J. J., and Mansour, A. E., 2002. Estimation of the long-term wave-induced bending moment
727 in ships using closed-form expressions. *International Journal of Maritime Engineering.* 144:41–
728 5.

729 Juncher, J. J. and Terndrup, P. P., 1979. Wave-induced bending moments in ships - a quadratic
730 theory. *Royal Inst Naval Architects Supplementary Papers.* 121:151–65.

731 Jung K., Lee S., Kim H., Choi Y., and Kang S., 2019. Design and construction of concrete floating
732 pier in golden harbor, Incheon. In: *Proceedings of World Conference on Floating Solutions 2019*,

733 vol 41. April 22-23, Singapore.

734 Kashiwagi, M., 1998a. A B-spline Galerkin scheme for calculating the hydroelastic re- sponse of
735 a very large floating structure in waves. *Journal of Marine Science and Technology*. 3:37–49.

736 Kashiwagi, M., 1998b. A hierarchical interaction theory for wave forces on a large number of
737 elementary bodies of a semi-sub type VLFS. *Proceedings of 14th ocean engineering symposium*.
738 425–31.

739 Kashiwagi, M., 2000. A time-domain mode-expansion method for calculating transient elastic
740 responses of a pontoon-type VLFS. *Journal of Marine Science and Technology*. 5:89–100.

741 Kashiwagi, M., 2004. Transient responses of a VLFS during landing and take-off of an airplane.
742 *Journal of Marine Science and Technology*. 9:14-23.

743 Khabakhpasheva, T., and Korobkin, A., 2002. Hydroelastic behaviour of compound floating plate
744 in waves. *Journal of Engineering Mathematics*. 44:21–40.

745 Kim, B., Hong, S., Kyoung, J. and Cho, S., 2007. Evaluation of bending moments and shear forces
746 at unit connections of very large floating structures using hydroelastic and rigid body analyses.
747 *Ocean Eng.* 34.

748 Kim, Y., and Kim, K., 2009. Analysis of hydroelasticity of floating shiplike structure in time
749 domain using a fully coupled hybrid BEM-FEM. *J Ship Res.* 50:31–47.

750 Koekoek, M.J., 2006. Connecting Modular Floating Structures: A General Survey and Structural
751 Design of a Modular Floating Pavilion. Master Thesis. Delft University of Technology.

752 Lakshmyanarayananana, P., and Temarel, P., 2019. Application of CFD and FEA coupling to predict
753 dynamic behaviour of a flexible barge in regular head waves. *Marine Structures*. 65:308-25.

754 Lee, C., and Newman, J.N., 2000. An assessment of hydroelasticity for very large hinged vessels.
755 *J Fluids Struct.* 14:957–70.

756 Lee, K. H., and Lee, P. S., 2016. Nonlinear hydrostatic analysis of flexible floating structures. *Appl.*
757 *Ocean Res.*; 59, 165–182.

758 Lee, S., Takaki, M. and Iwano, M., 2003. Estimation of the radiation forces on submerged-plate
759 oscillating near a free surface by composite grid method. *Trans West-Jpn Soc Nav Arch.* 105:113–
760 22.

761 Lei H. H., 2007. Securing of marine platforms in rough sea. *Recent Patents on Engineering*. 1:103-
762 112.

763 Li, J., Wu, Z., Shi, C., Yuan, Q., and Zhang, Z. 2020. Durability of ultrahigh performance concrete–

764 A review. *Construction and Building Materials*, 255, 119296.

765 Liu, C., 2014. Research on Structural Response of Multi-Module Flexible Connectors for Very
766 Large Floating Structures. Mater Thesis, China Ship Scientific Research Center, Wuxi, China.

767 Liu, C., Qi, E., Lu, Y., 2014. Dynamic response of connectors of Very Large Floating Structures
768 under shallow draft. *Journal of Ship Mechanics*. 18(05):581-590. (in Chinese)

769 Liu, X., and Sakai, S., 2002. Time domain analysis on the dynamic response of a flexible floating
770 structure to waves. *Journal of Engineering Mechanics*. 128:48–56.

771 Lotsberg, I. 2016. Fatigue design of marine structures. Cambridge University Press:
772 UK.Loukogeorgaki, E., Michailides, C. and Angelides, D., 2012. Hydroelastic analysis of a
773 flexible mat-shaped floating breakwater under oblique wave action. *J Fluid Struct*. 31:103-24.

774 Loukogeorgaki, E., Yagci, O. and Kabdasli, M., 2014. 3D Experimental investigation of the
775 structural response and the effectiveness of a moored floating breakwater with flexibly connected
776 modules. *Coastal Engineering*. 91:164-180.

777 Martinelli, L., Zanuttigh, B., and Ruol, P., 2008. Wave basin experiments on floating breakwaters
778 with different layouts. *Appl Ocean Res*. 30:199–207.

779 Mcallister K., 1997. Mobile offshore bases—An overview of recent research. *Journal of Marine
780 Sciences and Technology*. 2:173-181.

781 Michailides, C., Loukogeorgaki, E., and Angelides, D., 2013. Response analysis and optimum
782 configuration of a modular floating structure with flexible connectors. *Appl Ocean Res*. 43:112–
783 30.

784 Namba, Y., and Ohkusu, M., 1999. Hydroelastic behavior of floating artificial islands in waves.
785 *International Journal of Offshore and Polar Engineering*. 9:39–47.

786 Nematbakhsh, A., Gao, Z. and Moan, T., 2017. Benchmarking of a computational fluid dynamics-
787 based numerical wave tank for studying wave load effects on fixed and floating offshore structures.
788 *J Offshore Mech Arctic Eng*. 139:031301.

789 Newman, J.N., 1994. Wave effects on deformable bodies. *Appl Ocean Res*. 1994: 47–59.

790 Newman, J.N., 1997. Wave effects on hinged bodies. Part II –hinge loads.

791 Nguyen, H.P., Wang, C.M., Flocard, F., and Pedroso, D.M., 2019. Extracting energy while
792 reducing hydroelastic responses of VLFS using a modular raft WEC-type attachment. *Appl. Ocean
793 Res*. 84, 302–316

794 Ohkusu, M., and Namba, Y., 2004. Hydroelastic analysis of a large floating structure. *J Fluid Struct*.

795 19:543-55.

796 Ohmatsu, S. 2005. Overview: Research on wave loading and responses of VLFS. *Marine*
797 *Structures*, 18(2), 149-168.

798 Pantelides, C., Reaveley, L., McMullin, P. 2003. Design of CFRP Composite Connector for Precast
799 Concrete Elements. *Journal of Reinforced Plastics and Composites*. 22(15):1335-1351.

800 Peña, E., Ferreras, J., and Sanchez-Tembleque, F., 2011. Experimental study on wave transmission
801 coefficient, mooring lines and module connector forces with different designs of floating
802 breakwaters. *Ocean Eng.* 38:1150–60.

803 Qi, E., Liu, C., Xia, J., Lu, Y., Li, Z., Yue, Y., 2015. Experimental study of functional simulation
804 for flexible connectors of very large floating structure. *Journal of Ship Mechanics*. 19(10):1245-
805 1254.

806 Qi, E., Song, H., Li, Z., Zhang, H., Xia, J., Zhu, Y., 2017. S Model test of fatigue strength of a
807 flexible connector of very large floating structures. *Journal of Ship Mechanics*. 21(11):1374-1382.

808 Qi, E., Song, H., Lu, Y., Li, Z., Xia, J., 2017. Study on dynamic response of flexible connectors of
809 very large floating structures. *Proceedings of the Conference to Mark the 20th Anniversary of*
810 *Journal of Ship Mechanics*. 9:218-226 (in Chinese).

811 Rahman M. A., and McQuaker, T. 2016. “Application of ultra high performance concrete in
812 expediting the replacement and rehabilitation of highway bridges.” Proc., First Int. Interactive
813 Symp. on UHPC, Iowa State Univ., Des Moines, Iowa.

814 Ramsamooj, D. V. and Shugar, T. A., 2001. Prediction of fracture-based fatigue life of connectors
815 for the mobile offshore base. *Marine Structures*,2001,14(1): 197-214.

816 Ramsamooj, D. V. and Shugar, T. A., 2002. Reliability analysis of fatigue life of the connectors-
817 the US mobile offshore base. *Marine Structures*. 15:233–250.

818 Ren, N., Zhang, C., Magee, A.R., Hellan, Ø., Dai, J., and Ang, K.K., 2019. Hydrodynamic analysis
819 of a modular multi-purpose floating structure system with different outermost connector types.
820 *Ocean Eng.* 176, 158–168.

821 Riggs, H.R., and Ertekin, R.C., 1993. Approximate methods for dynamic response of multi-module
822 floating structures. *Marine Structures*. 6: 117-141.

823 Riggs H.R., Ertekin, R.C., and Mills, T., 1999. Impact of stiffness on the response of a multimodule
824 mobile offshore base. *International Journal of Offshore and Polar Engineering*. 9:126-33.

825 Riggs, H., Ertekin, R., and Mills, T., 2000. A comparative study of RMFC and FEA models for the

826 wave-induced response of a MOB. *Marine Structures*. 13:217–32.

827 Riyansyah, M., Wang, C.M. and Choo, Y.S., 2010. Connection design for two-floating beam
828 system for minimum hydroelastic response. *Marine Structures*. 23(1), 67-87.

829 Rognaas, G, Xu, J., Lindseth, S., and Rosendahl, F., 2001. Mobile offshore base concepts concrete
830 hull and steel topsides. *Marine Structures*. 14:5-23.

831 Sen, R., Shahawy, M., Rosas, J., Sukumar, S., 1998a. Durability of aramid pretensioned elements
832 in a marine environment. *ACI Struct J*. 95(5):578–87.

833 Sen, R., Shahawy, M., Rosas, J., Sukumar, S., Rosas, J. , 1998b. Durability of carbon pretensioned
834 elements in a marine environment. *ACI Struct J*. 95(6):716–24.

835 Senjanovic, I., Catipovic, I., and Tomasevic, S., 2008. Coupled horizontal and torsional vibrations
836 of a flexible barge. *Engineering Structures*. 30:93–109.

837 Senjanovic, I., Malenica, S., and Tomasevic, S., 2008a. Investigation of ship hydroelasticity.
838 *Ocean Engineering*. 35:523–35.

839 Senjanovic, I., Tomic, M., and Tomasevic, S., 2008b. An explicit formulation for restoring stiffness
840 and its performance in ship hydroelasticity. *Ocean Engineering*. 35:1322–38.

841 Shi, C., Wu, Z., Xiao, J., Wang, D., Huang, Z., and Fang, Z. 2015. A review on ultrahigh
842 performance concrete: part I. Raw materials and mixture design, *Constr. Build. Mater*. 101:741–
843 751.

844 Shi, Q., Xu, D., and Zhang, H., 2018. Design of a flexible-base hinged connector for very large
845 floating structures. *ASME 2018 37th International Conference on Ocean, Offshore and Arctic*
846 *Engineering*.

847 Suzuki, H., 2005. Overview of Megafloat: concept, design criteria, analysis, and design. *Mar.*
848 *Struct*. 18, 111–132.

849 Taylor, R., 2007. Wet hydroelastic analysis of plates and some approximations. *Journal of*
850 *Engineering Mathematics*. 58:267–78.

851 Teng, B., Gou, Y., Wang, G. and Cao, G., 2014. Motion response of hinged multiple floating bodies
852 on local seabed. *Proceedings of the Twenty-Fourth International Offshore and Polar Engineering*
853 *Conference (ISOPE 2014)*. Busan, South Korea; 591-8.

854 Wang, C., Fu, S., and Cui, W. 2009. Hydroelasticity based fatigue assessment of the connector for
855 a ribbon bridge subjected to a moving load. *Marine structures*, 22(2), 246-260.

856 Wang, C.M., Riyansyah, M., and Choo, Y. S., 2009. Reducing hydroelastic response of

857 interconnected floating beams using semi-rigid connections. *Proceedings of the ASME 28th*
858 *International Conference on Offshore Mechanics and Arctic Engineering*, May 31 - June 5,
859 Honolulu, Hawaii, USA, OMAE2009-79692.

860 Wang, C.M., and Tay, Z.Y., 2011. Very large floating structures: applications, research and
861 development. *Procedia Engineering*. 14:62-72.

862 Wang C.M. and Wang, B.T., 2015. Large Floating Structures: Technological Advances. Singapore:
863 Springer Singapore.

864 Wang, D., Shi, C., Wu, Z., Xiao, J., Huang, Z., and Fang, Z. 2015. A review on ultrahigh
865 performance concrete: part II. Hydration, microstructure and properties, *Constr. Build. Mater.* 96:
866 368–377.

867 Wang, D.Y., Riggs, H.R., Ertekin, R.C., 1991. Three-dimensional hydroelastic response of a very
868 large floating structure. *International Journal of Offshore and Polar Engineering*. 1:307–16.

869 Wang, P., Yu, L., Li, R., 2002. A time sequence analysis method for predicting connector loads in
870 a semi-submersible very large floating structure. *China Ocean Engineering*. 20(3):9-13. (in
871 Chinese)

872 Watanabe, E., Utsunomiya, T., and Tanigaki, S., 1998. A transient response analysis of a very large
873 floating structure by finite element method. *JSCE Structural Engrg/Earthquake Engrg*. 15:155–
874 63.

875 Watanabe E, Utsunomiya, T., and Wang, C. M., 2004. Hydroelastic analysis of pontoon-type VLFS:
876 a literature survey. *Engineering structures*. 26:245-56.

877 Wilkins D., 2002. Interlocking System, Apparatus and method for connecting modules." US patent
878 no. 6470820.

879 Wei, W., Fu, S., Moan, T., Liu, Z., and Deng, S., 2017. A discrete-modules-based frequency domain
880 hydroelasticity method for floating structures in inhomogeneous sea conditions. *Journal of Fluids*
881 *and Structures*, 74:321-339.

882 Wei, W., Fu, S., Moan, T., Song, C., and Ren, T., 2018. A time-domain method for hydroelasticity
883 of very large floating structures in inhomogeneous sea conditions. *Marine Structures*, 57:180-192.

884 Wu, C., Watanabe, E., and Utsunomiya, T., 1995. An eigenfunction expansion matching method
885 for analysis wave-induced response of a large floating plate. *Applied Ocean Research*. 17:301–10.

886 Wu, Y., and Cui, W., 2009. Advances in the three dimensional hydroelasticity of ships. *Proceedings*
887 *of the Institution of Mechanical Engineers, Part M: J Engng Maritime Environment*. 223:331-48.

888 Wu, Y., Maeda, H., and Kinoshita T., 1997. The second order hydrodynamic actions on flexible
889 body. Departmental Bulletin Paper, Institute of Industrial Science, the University of Tokyo.
890 49(4):190-201.

891 Xia, D., Kim, J., and Cengiz Ertekin, R., 2000. Review on Conceptual Designs and Key
892 Technologies of Very Large Floating Structures. *Journal of Ship Mechanics*. 24(6):135-148.

893 Xia, S., Xu, D., Zhang, H., Qi, E., Hu, J., and Wu, Y., 2016. On retaining a multi-module floating
894 structure in an amplitude death state. *Ocean Engineering*. 121:134-142.

895 Xie, Z., Gu, X., Ding, J., Zhao, N., and Hang, G., 2020. On retaining a multi-module floating
896 structure in an amplitude death state. *Ocean Engineering*. 121:134-142.

897 Xu, D., Zhang, H., Lu, C., Qi, E., Hu, J. and Wu, Y., 2014. On study of nonlinear network dynamics
898 of flexibly connected multi-module very large floating structures. *Vulnerability, Uncertainty, Risk*.
899 1805–14.

900 Yoon, D.G. and Boldbaatar, T., 2013. A Study on the connector of floating platform based on
901 concrete structures. *Journal of Korean Society of Marine Environment and Safety*. 19:37–44.

902 Yoon, J., Cho, S., Jiwinangun, R. G., and Lee, P., 2014. Hydroelastic analysis of floating plates
903 with multiple hinge connections in regular waves. *Marine Structures*. 36:65-87.

904 Yu, J., Dong, W., Dai, Y., 2006a. The Application of RMFC Model in the Three-Dimensional
905 Motion Response Calculation of New Concatenation Type Maritime Quay of Landing Stage. *Port*
906 *Engineering Technology*. 4: 1-4. (in Chinese)

907 Yu, J., Su, C., 2006b. Research on motion ability calculation method of offshore moving trestle.
908 *China Harbour Engineering*. 146(6): 14-17. (in Chinese)

909 Yu, L., Ding, W., Li, R., 2004. Effect of the multiple modules interaction on MOB connector loads.
910 *China Ocean Engineering*. 37(8): 1159-1163. (in Chinese)

911 Yu, L., Li, R., Lu, Y., 2003. Dynamic Characteristics of Mobile Offshore Base Connectors. *Journal*
912 *of Shanghai Jiaotong University*. 37(8): 1159-1163. (in Chinese)

913 Yuan, J., and Graybeal, B. 2016. Full-scale testing of shear key details for precast concrete box-
914 beam bridges. *J. Bridge Eng.*, 10.1061/(ASCE)BE.1943-5592.0000906, 04016043.

915 Zhao, C., Hao, X., Liang, R., and Lu, J., 2015. Influence of hinged conditions on the hydroelastic
916 response of compound floating structures. *Ocean Eng.* 101:12-24.

917 Zhang, H., Qi, E., Song, H., Li, Z., Xia, J., 2019. Study on mechanical property of connector with
918 flexible sandwich of very large floating structures. *Journal of Ship Mechanics*. 23(02):200-210.

919 Zhang, H.C., Xu, D.L., Ding, R., Zhao, H., Lu, Y., and Wu, Y.S., 2019. Embedded Power Take-
920 Off in hinged modularized floating platform for wave energy harvesting and pitch motion
921 suppression. *Renew. Energy* 1176–1188.

922 Zhao, N., Gu, X., Qi, E., Li, S., Tang, M., 2018. Theoretical and experimental study on the ultimate
923 strength of the VLFS connector foundation support reinforcing area structure under complex loads.
924 *Journal of Ship Mechanics*. 22(07):857-864.

925 Zhao, H., Xu, D., Zhang, H., Xia, S., Shi, Q., Ding, R., and Wu, Y., 2019. An optimization method
926 for stiffness configuration of flexible connectors for multi-modular floating systems. *Ocean*
927 *Engineering*. 181:134–44.

928

Table 1. Results of Combined Compliant Connectors on Sides of Floating Module (De Rooij, 2006)


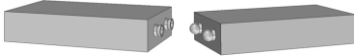

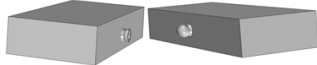
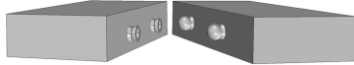
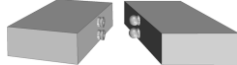
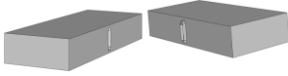
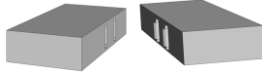
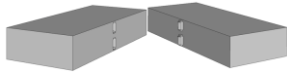






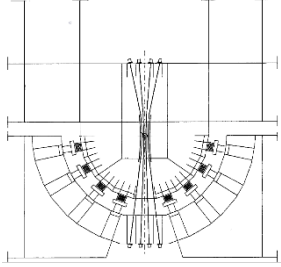
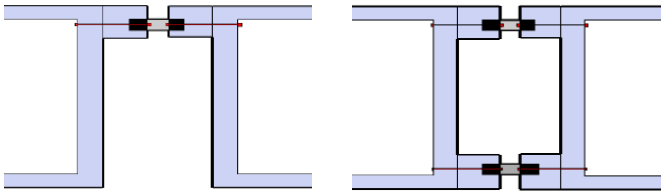
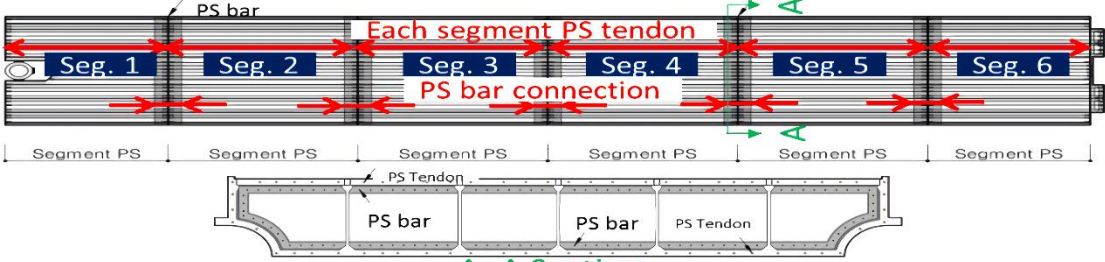
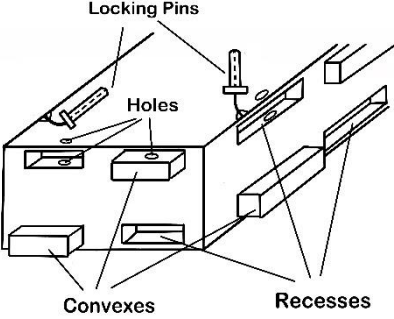
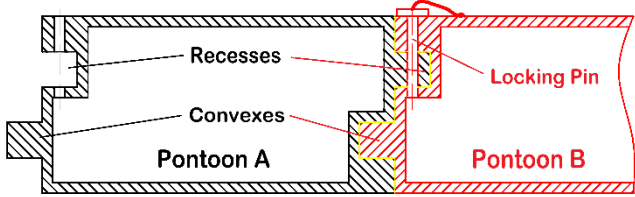
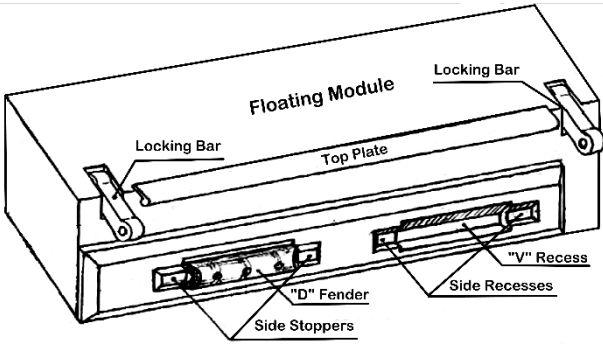
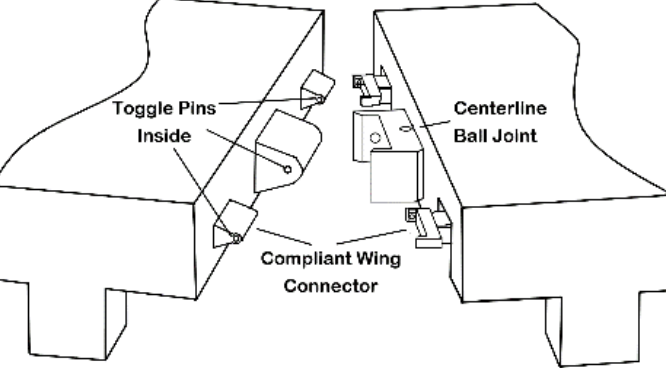
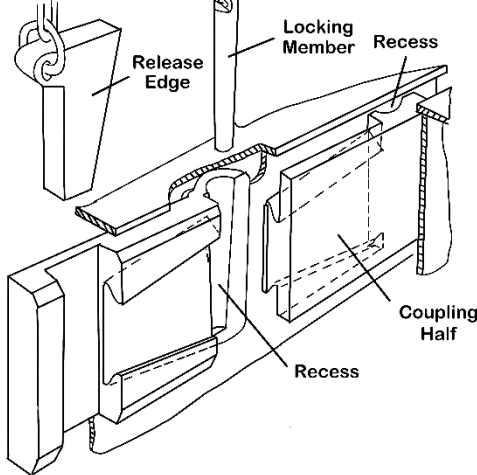
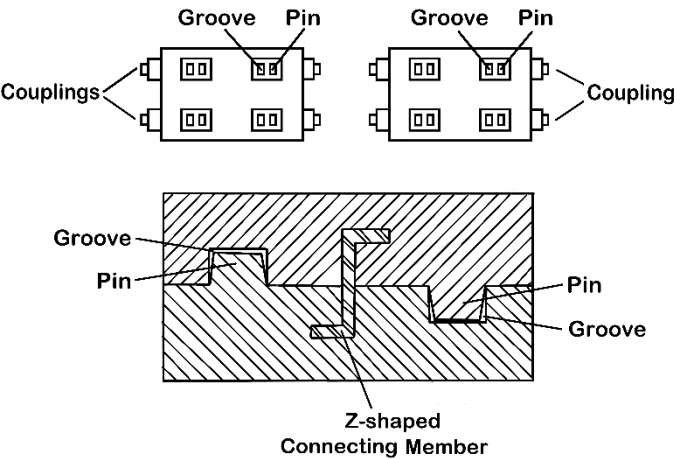
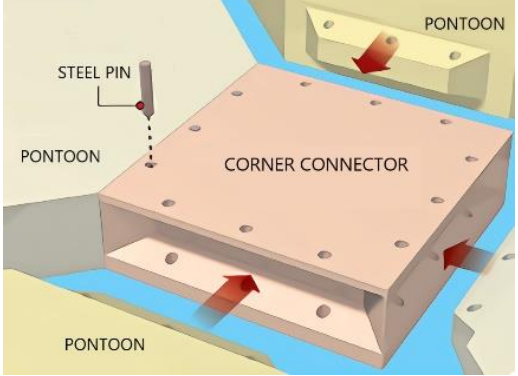
Type & Direction of connector	Allowed DOF by 1 connector	Extra restrained DOF.	
		2 hinges, (hor.) next to each other	2 hinges, (vert.) above each other
Centre point short face	all rotations 	roll, yaw 	pitch 
Centre point long face	all rotations 	pitch, yaw 	roll 
Vertical element long face	yaw 	yaw 	- 
Horizontal element short face	pitch 	yaw 	pitch 
Horizontal element long face	roll 	yaw 	roll 

Table 2. Positive and Negative Aspects of Rigid and Flexible Connector Systems

Type	Positive Aspects	Negative Aspects
Rigid Connector System	<ul style="list-style-type: none">• Small or no motions• Easy internal transport of containers• Complies with crane track requirements	<ul style="list-style-type: none">• Large connection forces• Complex connection configuration• Difficult to decouple the connectors
Flexible Connector System	<ul style="list-style-type: none">• Low connection forces• Easy decoupling process	<ul style="list-style-type: none">• Large motion amplitude• Complex internal transport• Flexible platform deck

Table 3. Rigid Connector Systems Developed with Different Design Principles

Principles	Typical Examples	Advantages	Disadvantages
Cable "Tensioning"	<div style="display: flex; justify-content: space-around;"> <div style="text-align: center;">  <p>a. Rognaas' Design</p> </div> <div style="text-align: center;">  <p>b. Halim's Design</p> </div> </div> <div style="text-align: center; margin-top: 20px;">  <p>c. Incheon Floating Pier</p> </div>	<ol style="list-style-type: none"> 1. Well distributed connection forces 2. Low cost 3. Adjustable connection stiffness 	<ol style="list-style-type: none"> 1. Weakness in shear aspects from heave motions 2. Vulnerable against corrosion 3. Difficult to disassemble
Hinge "Clicking"	<div style="display: flex; justify-content: space-around;"> <div style="text-align: center;">  </div> <div style="text-align: center;">  <p>d. Armin's Design</p> </div> </div>	<ol style="list-style-type: none"> 1. Well transferred forces 	<ol style="list-style-type: none"> 1. Relatively expensive 2. Easily damaged 3. Difficult for inspection or maintenance 4. Expensive to disassemble

	 <p>e. Han's Connector</p>	 <p>f. McDermott's MOB Connection</p>		
Tooth "Anchoring"	 <p>g. Bargeco's Design</p>	 <p>h. Gardner's Design</p>	<ol style="list-style-type: none"> 1. Bear high loads 2. Easy to disassemble 3. Not vulnerable 	<ol style="list-style-type: none"> 1. Accurate installation job needed 2. Margins required during coupling
	 <p>i. Marina Bay Float</p>			

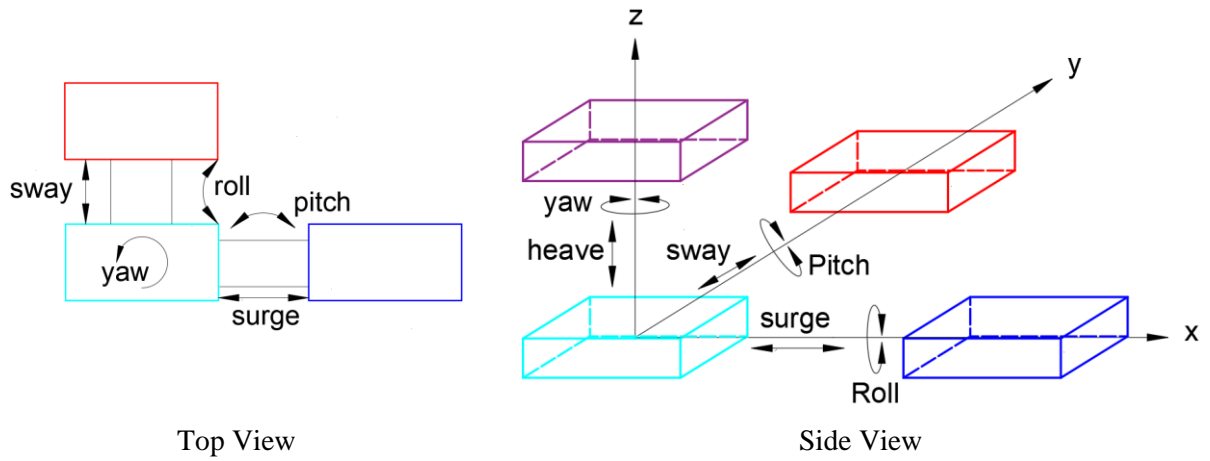
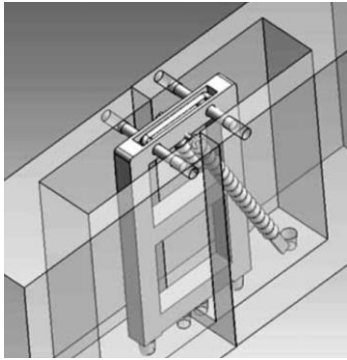
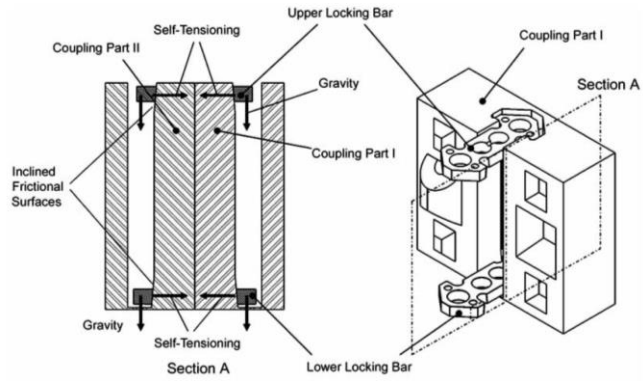


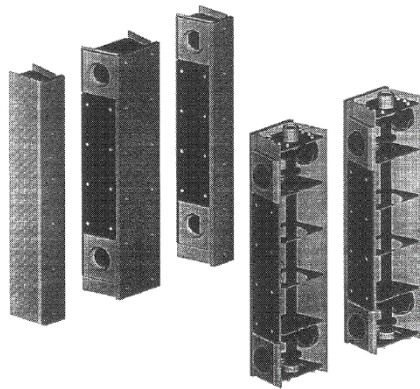
Figure 1. Relative Motions of Connected Floating Modules.



(a) Au-Yeong's Design (Yoon and Boldbaatar, 2013)

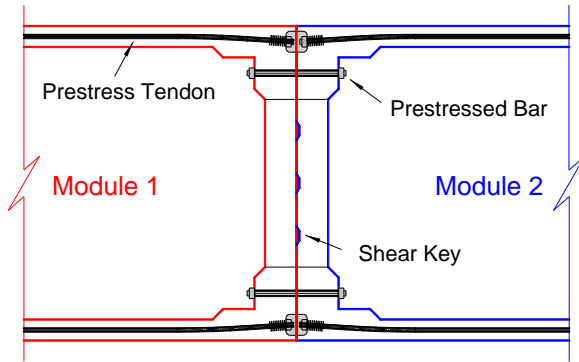


(b) Han's Frictional Locking Connector (Yoon and Boldbaatar, 2013)

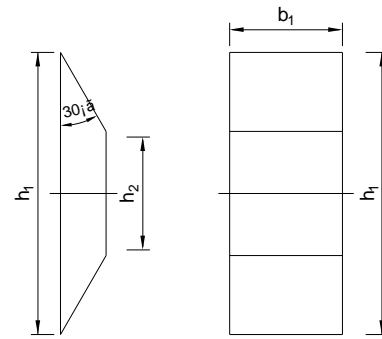


(c) Wilkins's Connector System (Wilkins, 2002)

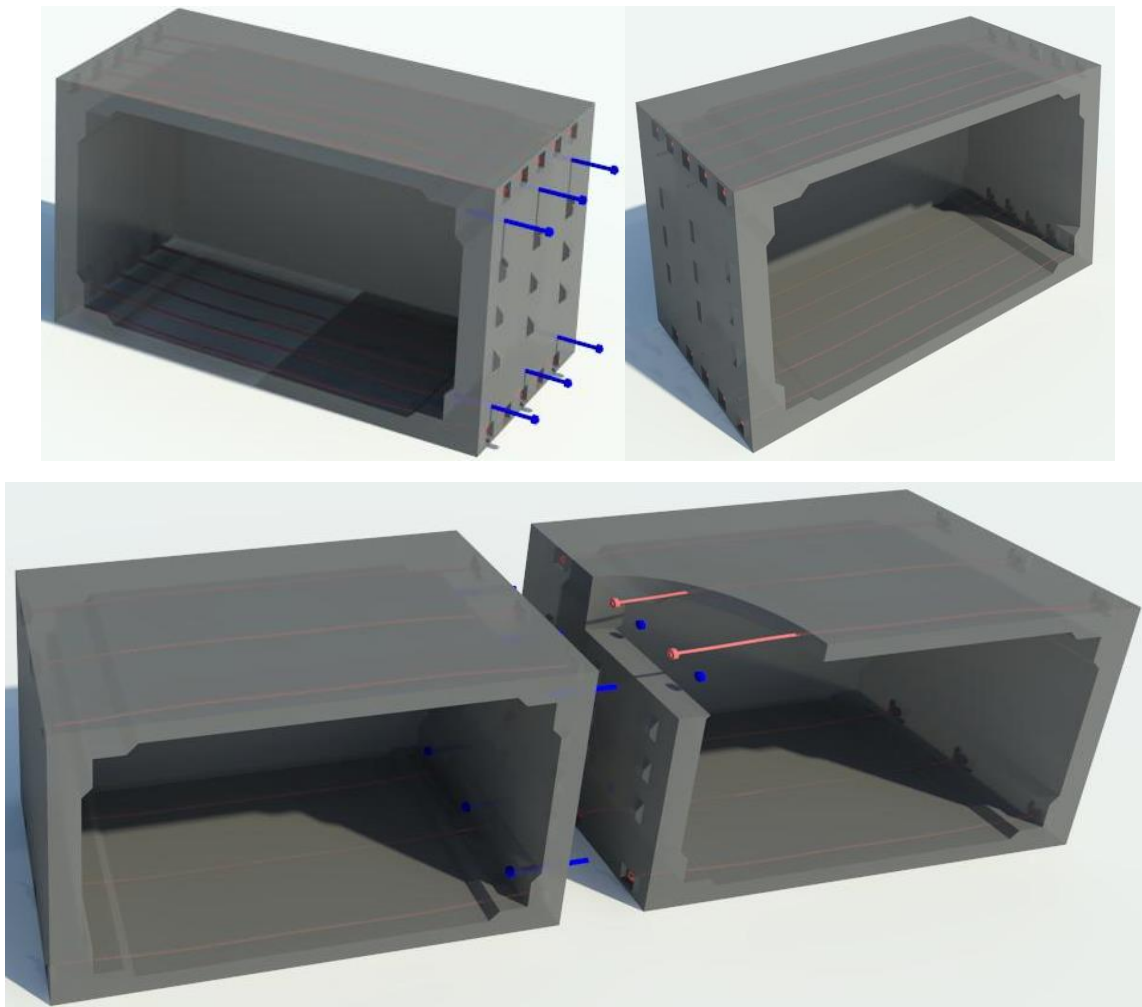
Figure 2. Connector Systems Using Bolts or Bars.



(a) Sectional View



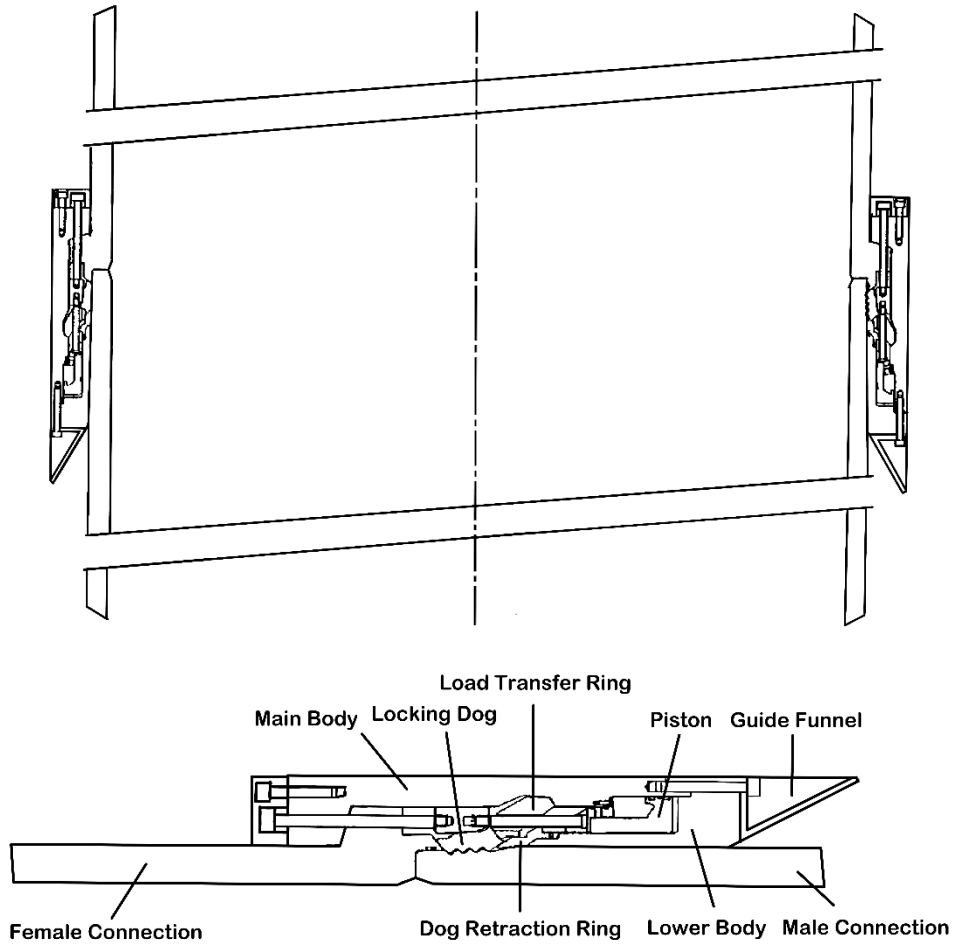
(b) Shear Key



(c) Three-dimensional View of Inter-connected Floating Module
Figure 3. Prestressed Concrete Shear Key Connection.

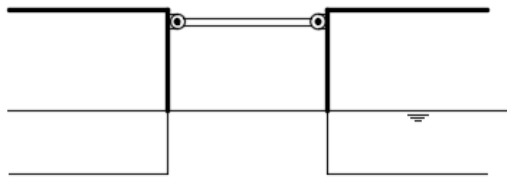


(a) Rigidly connected semi-submersible modules of MOB

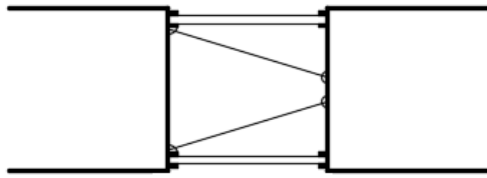


(b) ABB Vetco Grey latching system for connector

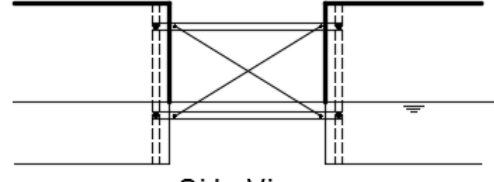
Figure 4. Rigid Connector System for MOB Proposed by Brown and Root (Ramsamooj and Shugar, 2002).



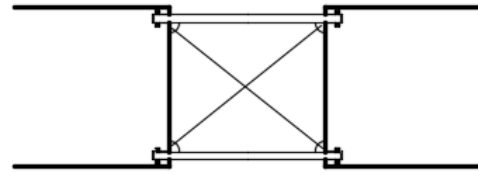
Side View



Top View



Side View



Top View

(a) "Rotation Allowing" Connection

(b) "Rotation Restricting" Connection

Figure 5. Vertical-free Connector Systems (Koekoek, 2006).

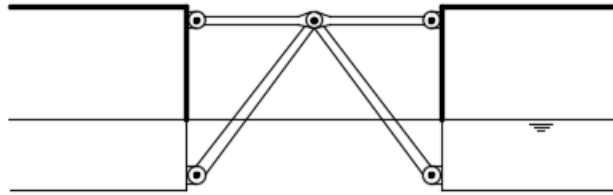


Figure 6. Hinge Connector Systems (Koekoek, 2006).

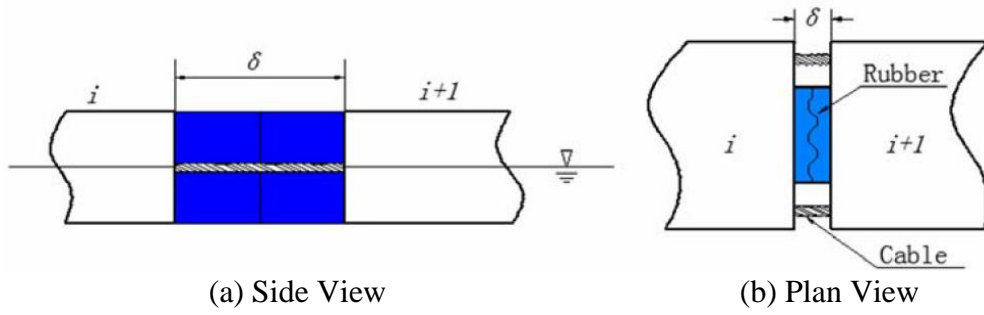


Figure 7. Rubber-Cable Connector System (Xu et al. 2014).

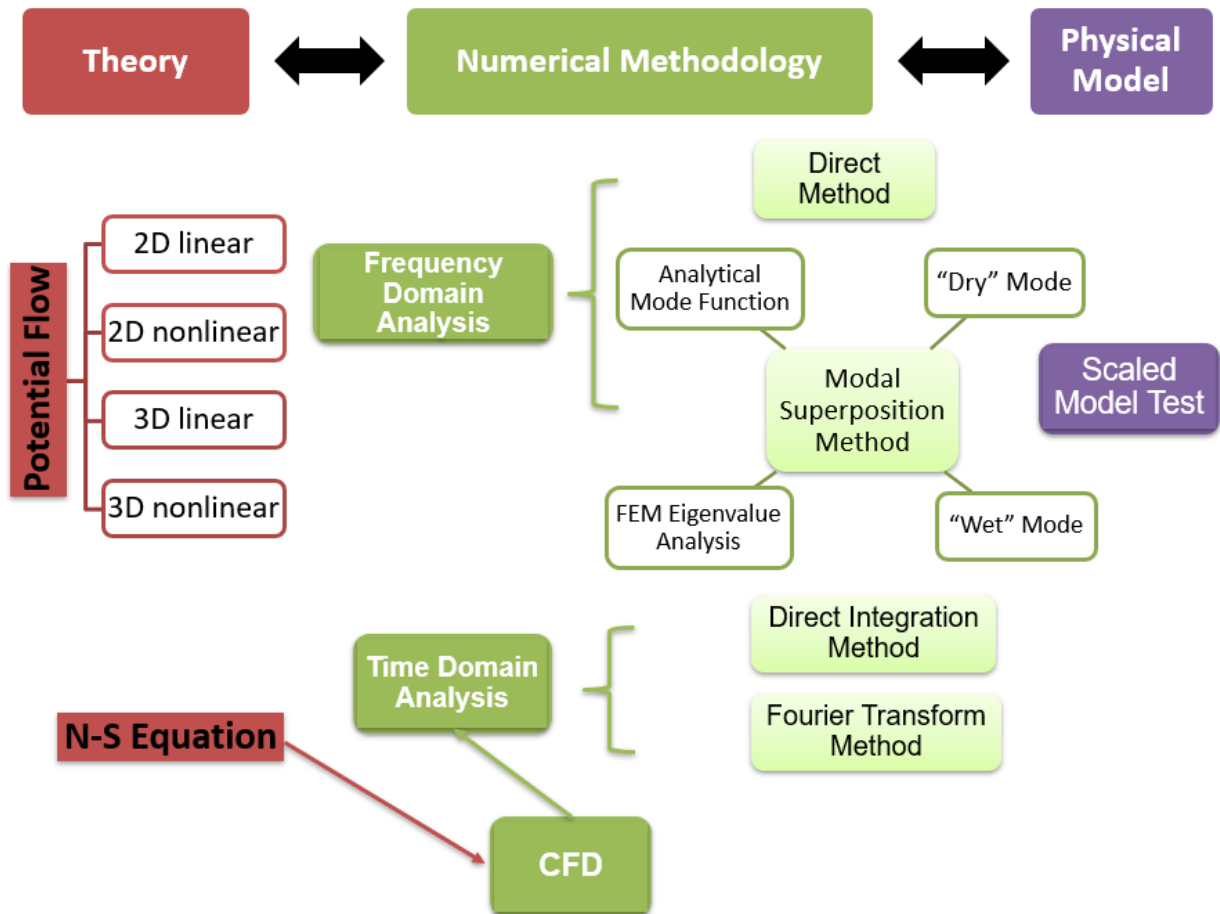
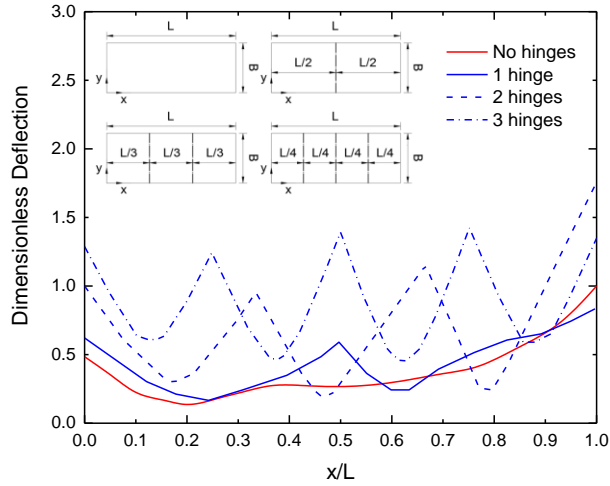
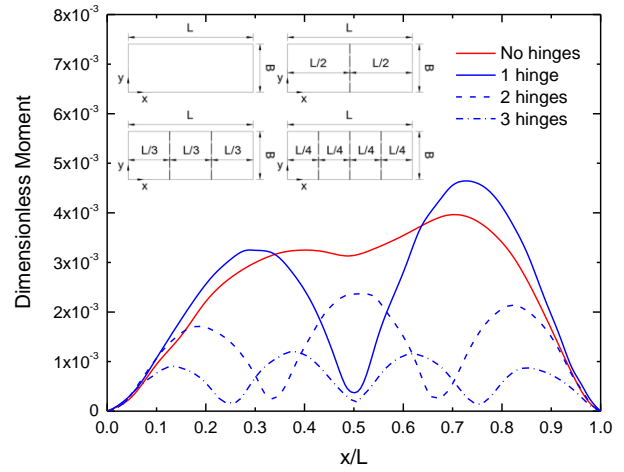


Figure 8. System of Numerical Methods for Hydroelastic Analysis.



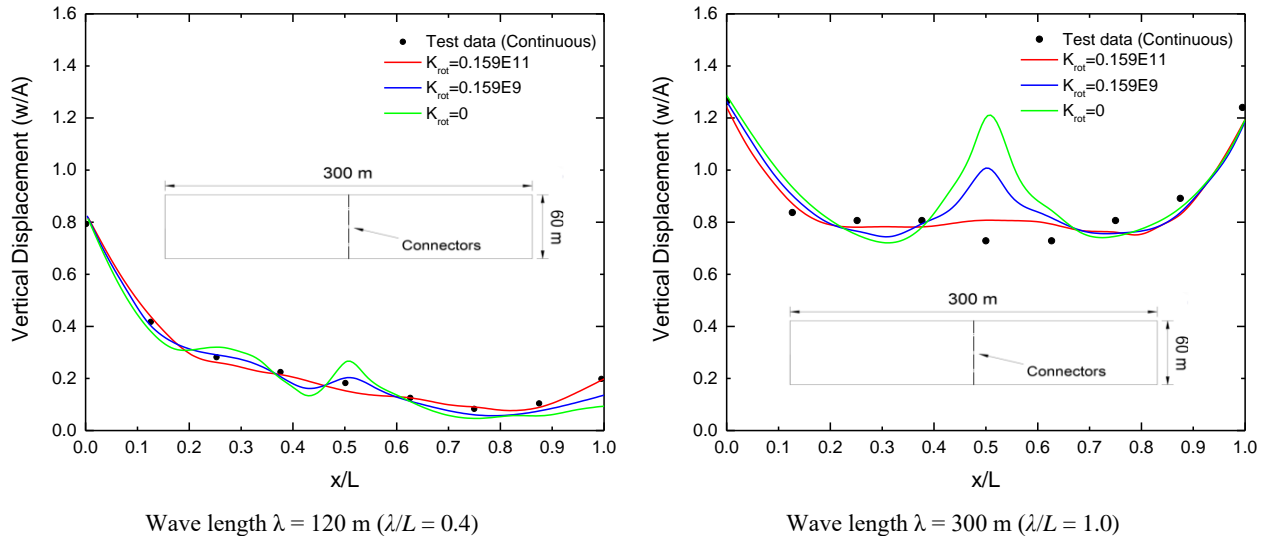
(a) RAOs of dimensionless vertical deflection



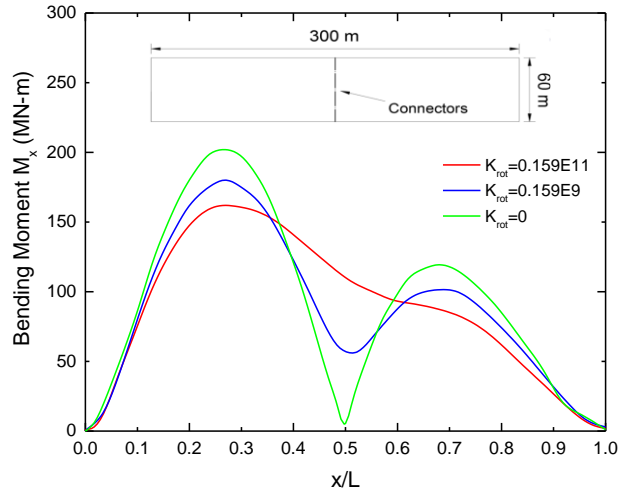
(b) RAOs of dimensionless bending moment

Note: Response amplitude operators (RAOs) of the dimensionless bending moment and deflection are defined as follows: $\bar{M}_{yy} = |M_{yy}| / \rho_w g L^2$ and $\bar{u}_3 = |u_3| / a$, where M_{yy} is the RAO of the bending moment per unit width, L is the length of floating plate, u_3 is the vertical deflection and a is the distance between two adjacent reflective markers ($a = 0.42$ m in Yoon et al. (2014)).

Figure 9. Hydroelastic Responses of Floating Plates with Multiple Hinge Connections in Head Sea (Adapted from Yoon et al. (2014)).



(a) Vertical displacements with different wave length



(b) Bending moment

Figure 10. Effects of Rotational Stiffness on Hydroelastic Response of Floating Modules Interconnected with Flexible Connectors with Varying Rotational Stiffness (Adapted from Fu et al. (2007)).

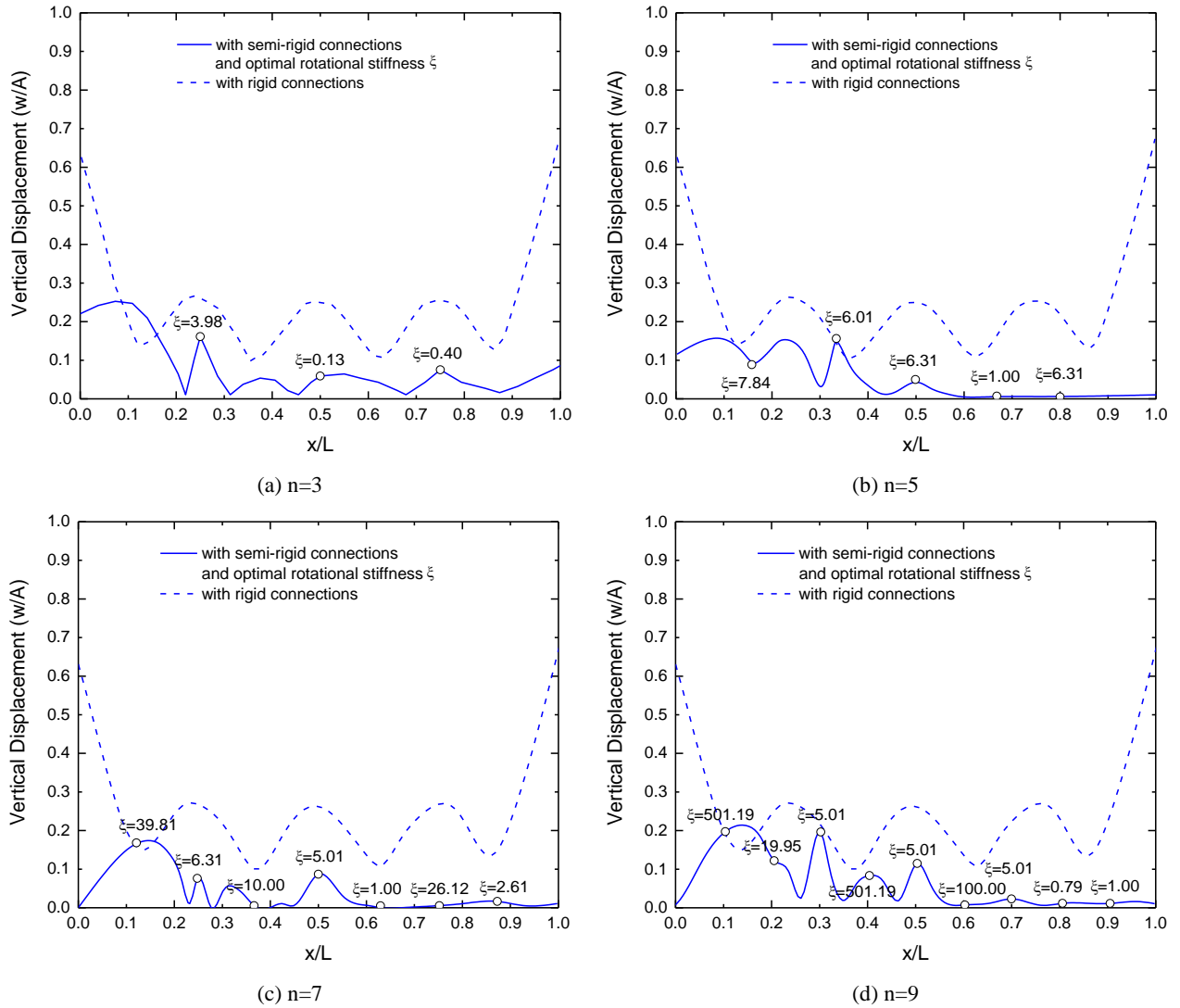
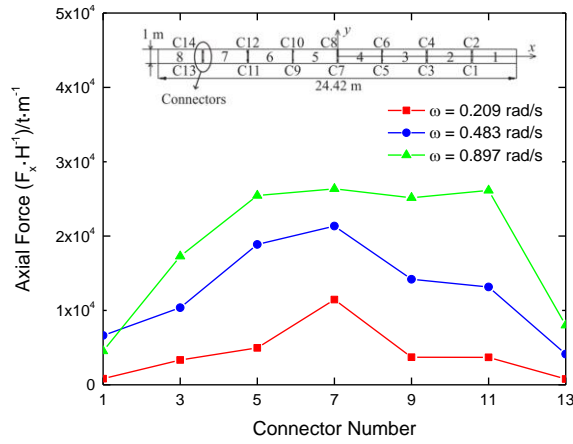
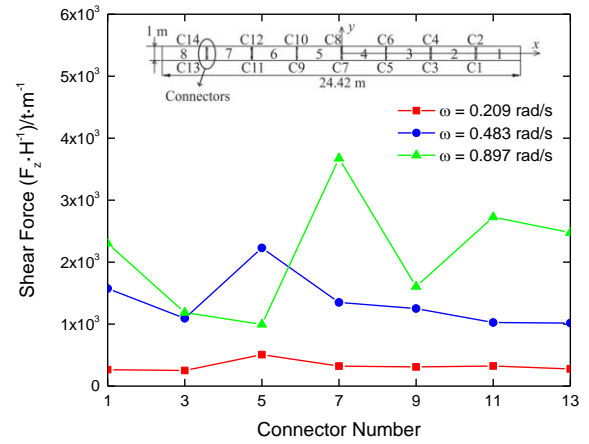


Figure 11. Hydroelastic Responses of Floating Beam with Optimum Locations and Optimum Rational Stiffness for (a) $n=3$, (b) $n=5$, (c) $n=7$, and (d) $n=9$. Structural Length $L = 300$ m, Water Depth $H = 20$ m (Adapted from Wang et al. (2009)).

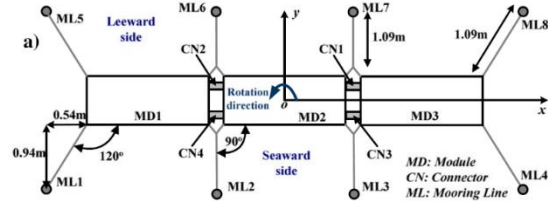


(a) Axial Force F_x

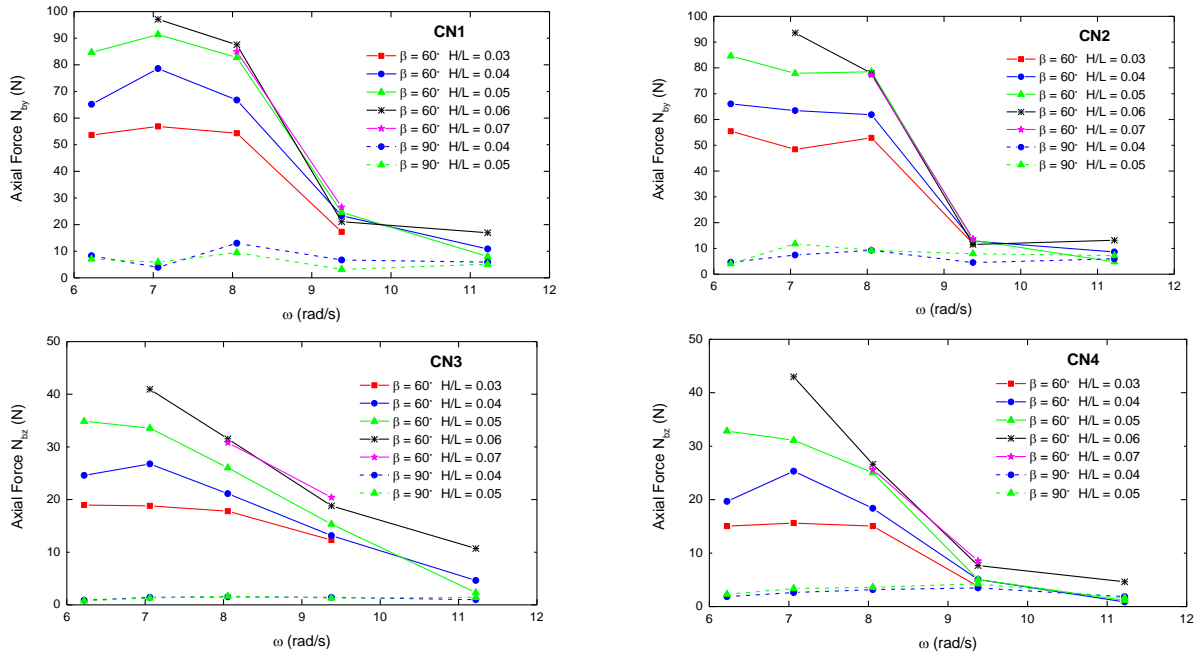


(b) Shear Force F_z

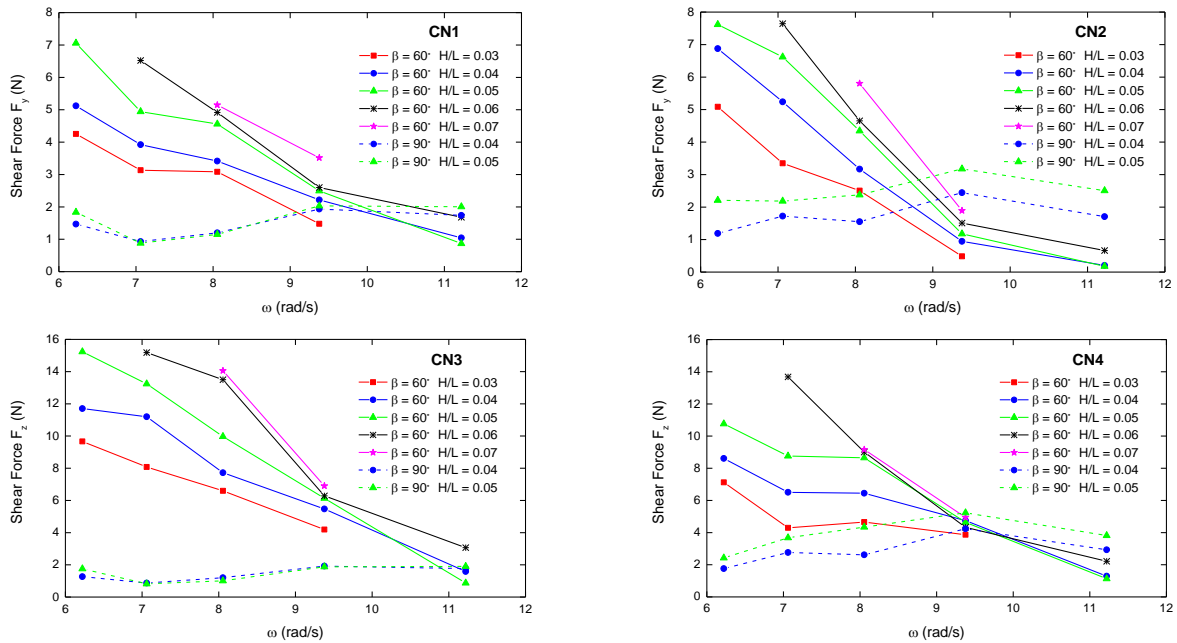
Figure 12. Variation of Connecting Forces along Length of Longish VLFS from C1 to C13 (Adapted from Ding et al. (2019)).



(a) Interconnected Floating Modules



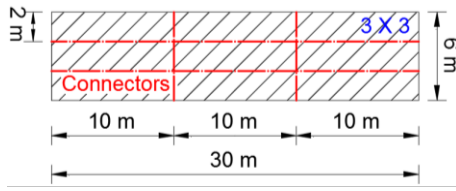
(b) Axial Forces



(c) Shear Forces

Note: H/L represents the wave steepness, where H is the incident wave height and L is the wave length.

Figure 13. Variation of Axial Forces and Shear Forces of CN1-CN4 as a Function of Incident Wave Frequencies (Adapted from Loukogeorgaki et al. (2014)).



FS _{ij} (3×3)	
Case	K _{Rj} (Nm/rad)
FS ₃₁	0
FS ₃₂	1.0E+3
FS ₃₃	1.0E+5

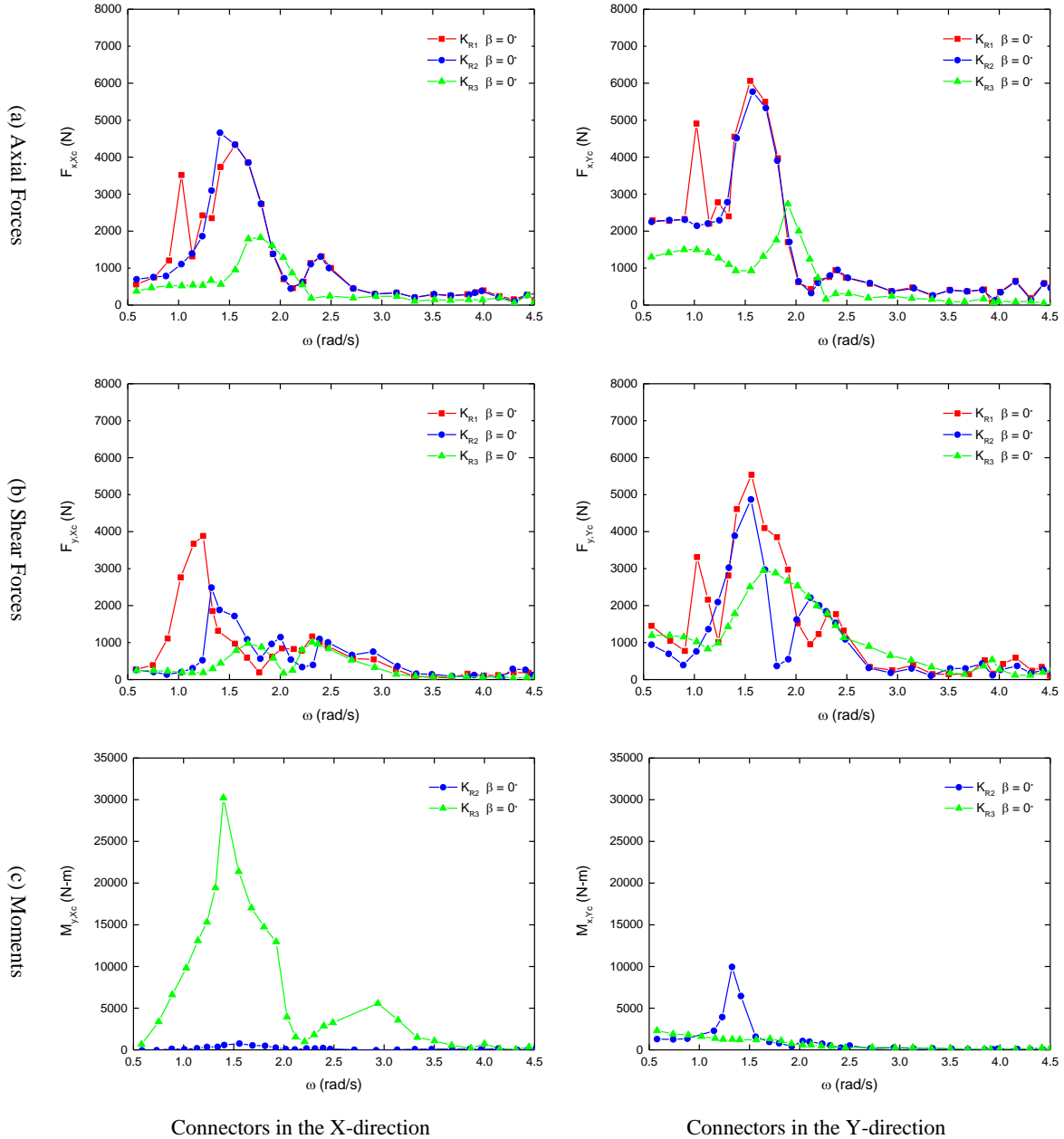


Figure 14. Connectors' Internal Forces of 3×3 Grid Type Floating Structures for Wave Angle $\beta = 0^\circ$ (Adapted from Michailides et al. (2013)).

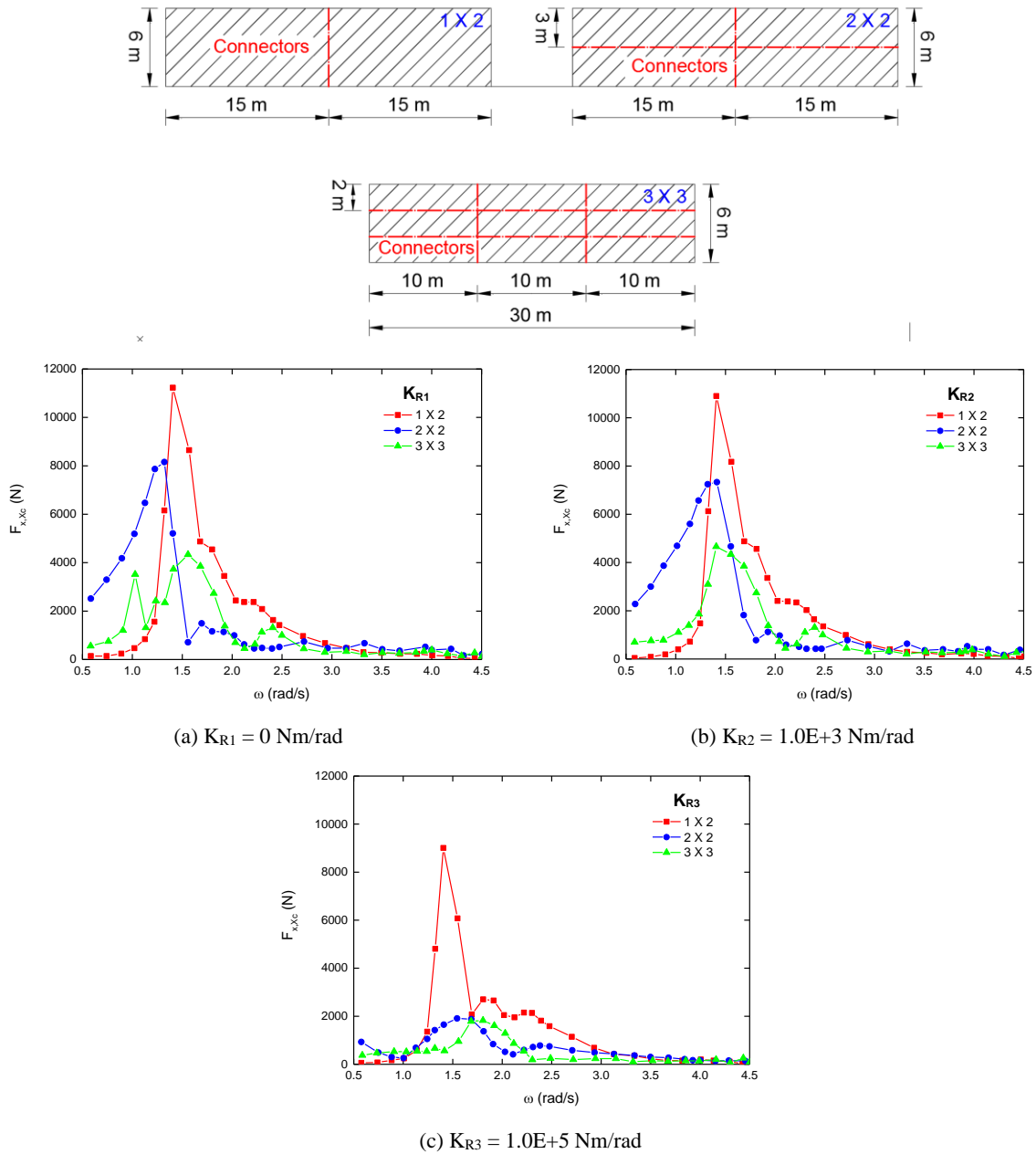
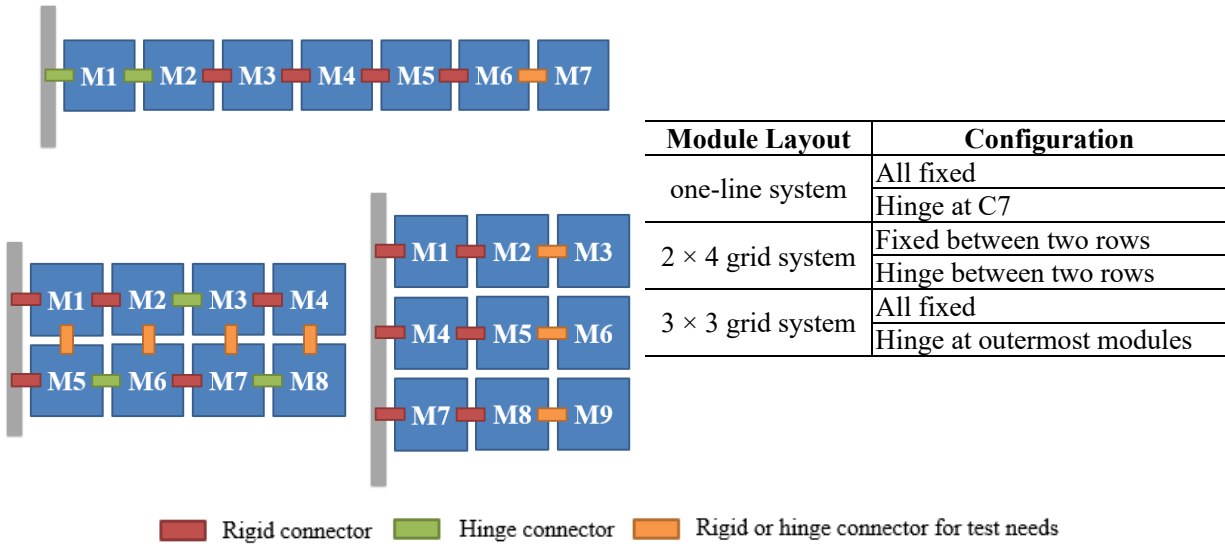
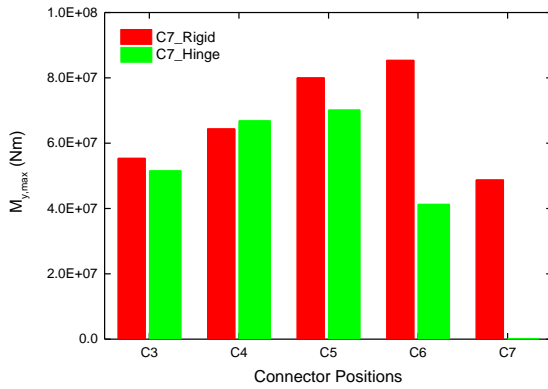


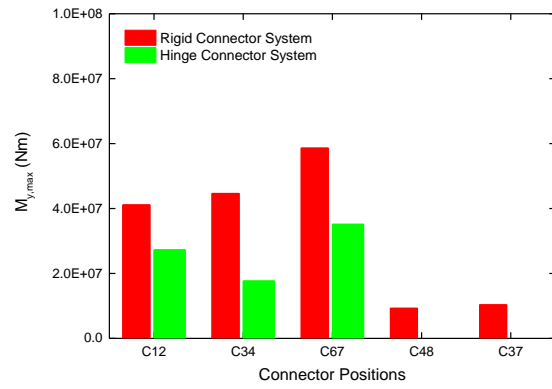
Figure 15. Variation of Connectors' Axial Forces in the X-direction for Different Module Layouts (Adapted from Michailides et al. (2013)).



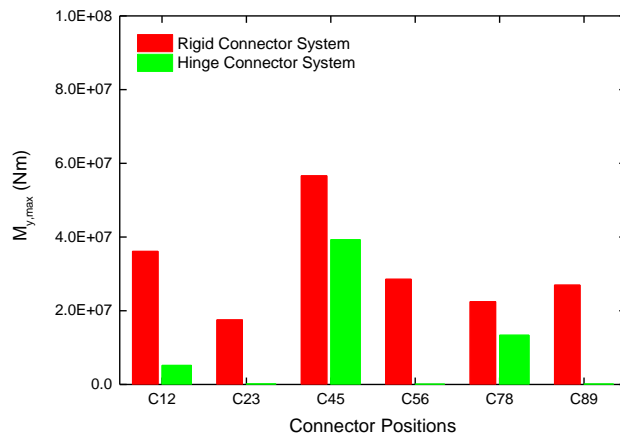
(a) Test module layout and connector arrangement



(b) One-line layout

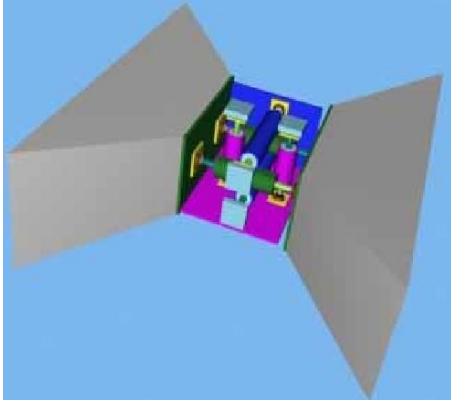


(c) 2 × 4 grid layout

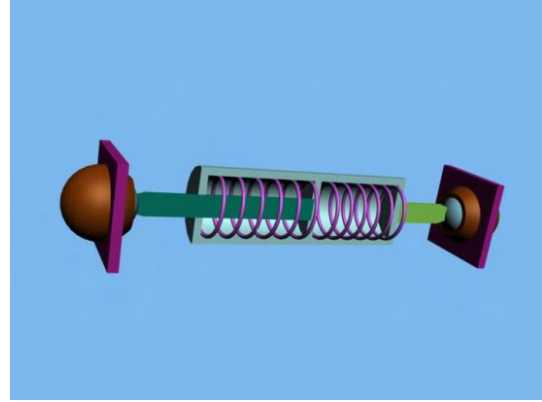


(d) 3 × 3 grid layout

Figure 16. Maximum Bending Moments of Floating Structures with Various Module Layouts and Different Combination of Hinge and Rigid Connectors.



(a) Connector configuration



(b) Ball and spring device

Figure 17. Flexible Connector System Proposed by Qi et al. (2015)

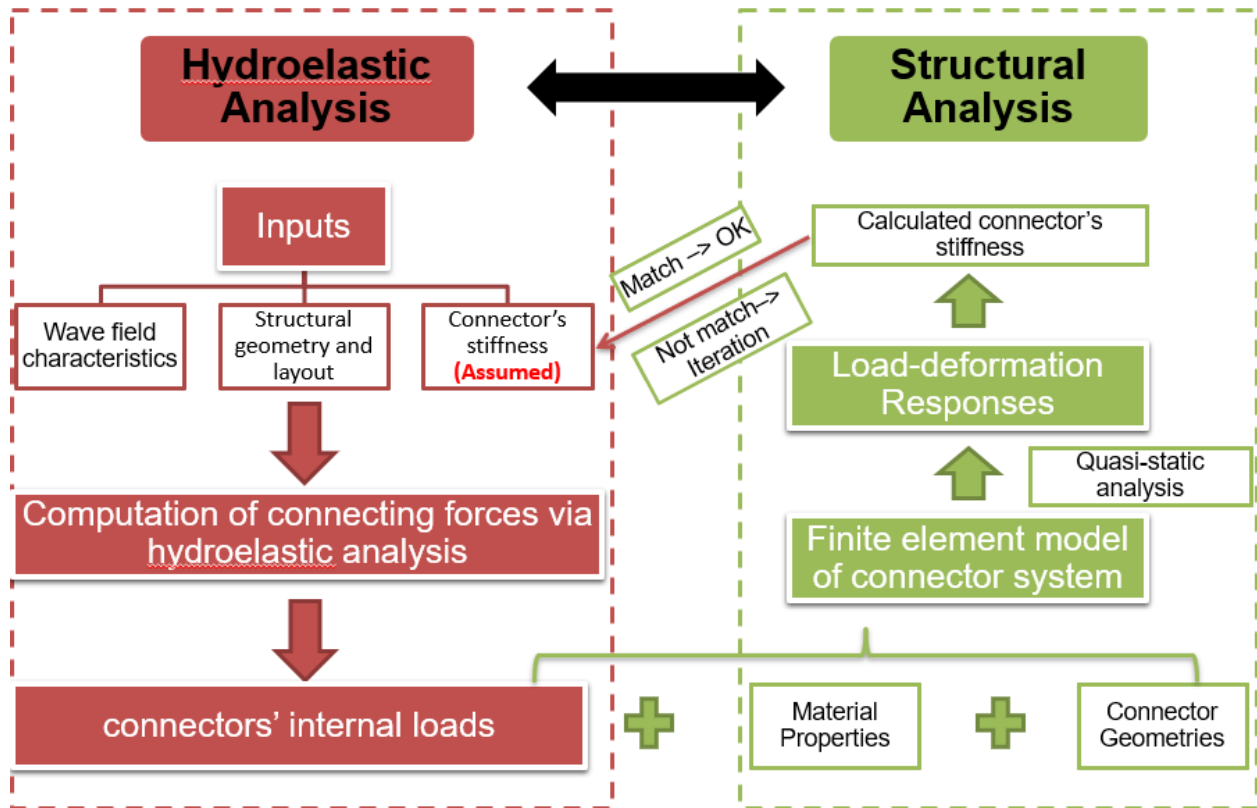
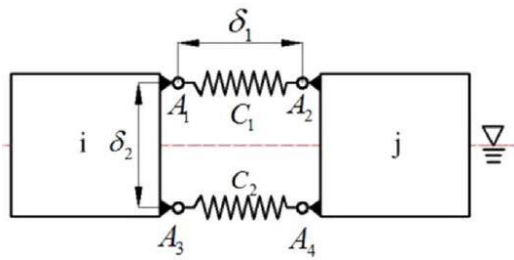
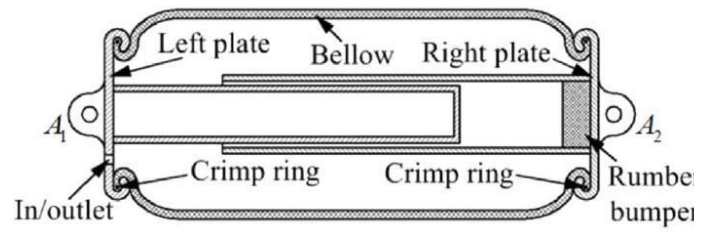


Figure 18. Flow of Determining Connector's Stiffness in Design Practice.



(a) Connection between adjacent modules



(b) Air-spring connector

Figure 19. Active-control Connector System Proposed by Xia et al. (2016)